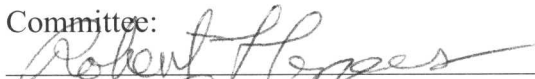


DEVELOPMENT AND ANALYSIS OF SELF-DECONTAMINATING COATINGS

by

Jeffrey G. Lundin
A Thesis
Submitted to the
Graduate Faculty
of
George Mason University
in Partial Fulfillment of
The Requirements for the Degree
of
Master of Science
Chemistry

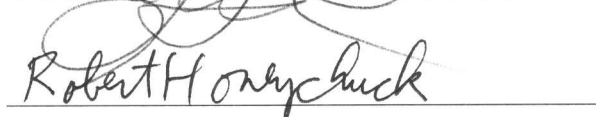
Committee:



Dr. Robert Cozzens, Thesis Director



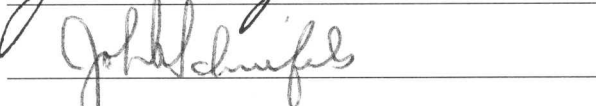
Dr. Gerald Roberts Weatherspoon,
Committee Member



Dr. Robert Honeychuck, Committee
Member



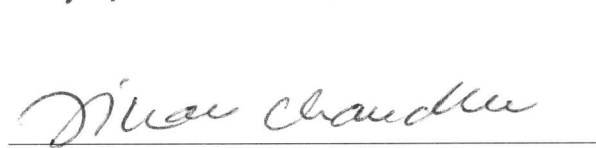
Dr. James Wynne, Committee Member



Dr. John Schreifels, Department
Chairman



Dr. Richard Diecchio, Associate Dean
For Academic and Student Affairs,
College of Science



Dr. Vikas Chandhoke, Dean, College
of Science

Date: 5/4/11

Spring Semester 2011
George Mason University
Fairfax, VA

Development and Analysis of Self-Decontaminating Coatings

A thesis submitted in partial fulfillment of the requirements for the degree of Master of Science at
George Mason University

By

Jeffrey George Lundin
Bachelor of Science
University at Albany, 2007

Director: Robert F. Cozzens, Professor
Department of Chemistry

Spring Semester 2011
George Mason University
Fairfax, VA

Copyright © 2011 by Jeffrey G. Lundin
All Rights Reserved

Dedication

This thesis is dedicated to my parents, George and Suzanne Lundin, for their continuous love and support.

Acknowledgments

I would like to thank Dr. Robert Cozzens for offering his invaluable guidance and comprehensive knowledge throughout my research. I owe a debt of gratitude to Dr. James Wynne whose resources, motivation, and infinite advice allowed me to accomplish this work. I would also like to acknowledge the exceptional insight and expertise provided by the members of my thesis committee, Dr. Gerald Roberts Weatherspoon and Dr. Robert Honeychuck.

I owe a special thanks to Dr. Preston Fulmer for his contributions to the improvement in both writing and presenting of my research. Mrs. Kelly Watson's expertise in gas chromatography-mass spectroscopy was essential in this work. Gratitude is owed for the support and assistance of Mr. Collin Bright and Mr. Nick Weise. Also, I greatly appreciate the sacrifice of Mr. Joe Buckley, whose summer days were devoted to the measurement of contact angle.

This research would have been impossible without the synthetic abilities of Dr. Brian Rasley and Mr. Spencer Giles at the University of Alaska Fairbanks. I would like to extend infinite thanks for the financial support of the Defense Threat Reduction Agency and the Office of Naval Research.

Table of Contents

	Page
List of Tables	vii
List of Figures	viii
List of Abbreviations	ix
Abstract	xi
1. Background	1
1.1 Introduction	1
1.2 Terminology	3
1.3 CWA Classification	4
1.4 Vesicants	7
1.5 Nerve Agents	11
1.6 Historical use of CWA	17
1.6.1 World War I	17
1.6.2 Nerve Agent Development	19
1.6.3 Terrorist Threat	21
1.7 CWAs of Interest	23
1.8 Decontamination Solutions	23
1.9 CWA Simulants	26
1.10 Polyurethane Coatings	29
1.11 Recent Research in Novel Reactive Systems	30
1.12 Selection of Reactive Coating Additives	31
2. Results and Discussion	37
2.1 Overview of Experimental Approach	37
2.2 Down-selection	38
2.3 Coating Characterization	40
2.3.2 Differential Scanning Calorimetry	45
2.4 Simulant Degradation on Fullerene Containing Coatings	48
2.4.1 Effects of light on fullerene coatings	49
2.4.2 Effects of specific spectral regions of light on fullerene coatings ..	53
2.4.3 By-product analysis of simulant degradation on fullerene coatings	56
2.4.4 Simulant degradation on coatings modified with CD	58
2.4.5 Simulant degradation on coatings modified with POMs	61
2.4.6 Effects of light on CD & POM modified coatings	62

2.4.7	Effects of atmospheric oxygen.....	65
3.	Conclusion	67
4.	Experimental Methods.....	68
4.1	Experimental Overview	68
4.2	Coating Preparation	68
4.3	Chemical Decontamination Challenge	69
4.4	GC/MS Analysis.....	70
4.5	UV-Vis Irradiation.....	71
4.6	Differential Scanning Calorimetry.....	72
4.7	Contact Angle Analysis	72
4.8	Nitrogen Purging.....	73
	References.....	74

List of Tables

Table	Page
1.1 NATO codes for chemical agents.....	3
1.2 Physical properties of HD (6).....	9
1.3 Toxicities of nerve agents.....	13
1.4 Physical properties of GA (7), GB (8), and GD (9).....	15
1.5 Physical properties of VX (10).....	16
1.6 Physical properties of HD compared with simulants.....	28
2.1 Chemical formulas of the additives screened.....	39
2.2 Contact angles and calculated surface energies of various coatings.....	43
2.3 Glass transition temperatures of formulated coatings.....	47
2.4 Reduction of simulants in dark and light conditions on fullerene coatings. ^a	50
2.5 Percent reduction of Demeton-S in variable light conditions on fullerene loaded coatings under isothermal conditions. ^a	55
2.6 Observed oxidation products of Demeton-S on fullerene loaded coatings under various light conditions given as the percent abundance of total products.....	58
2.7 Simulant reduction on coatings modified with cyclodextrin. ^a	59
2.8 Simulant reduction on POM modified coatings. ^a	61
2.9 Percent reduction of 2-CEPS and Demeton-S by CD and POM modified coatings in dark and light conditions at 24 hours. ^a	63
2.10 Reduction of Demeton-S on CD and POM coatings in various light conditions at 5.5 hours. ^a	64

List of Figures

Figure	Page
1.1 Structure of CS (1).....	5
1.2 Structure of phosgene (3).....	6
1.3 Structure of the incapacitating agent BZ (4).....	7
1.4 Structures of vesicants Lewisite (5) and HD (6).....	8
1.5 Formation of sulfonium ion from 6.....	10
1.6 Phosphorylation of the active site of AChE by a nerve agent. ³¹	11
1.7 Structures of GA (7), GB (8), and GD (9).....	14
1.8 Structures of VX (10) and VR (11).....	16
1.9 Structures of HD simulants 2-chloroethyl ethyl sulfide (12) and 2-chloroethyl phenyl sulfide (13).....	27
1.10 Structures of VX (10), Demeton-S (14) and Malathion (15).....	29
1.11 Absorption spectrum of fullerene in benzene.....	32
1.12 Truncated cone shape of cyclodextrin.....	34
1.13 General structure of cyclodextrin (CD) additives.....	35
2.1 Image of a contact angle measurement.....	41
2.2 DSC overlay of 5 (black line) and 10 (red line) % ^{w/w} fullerene coatings.....	46
2.3 Emission spectrum of the mercury vapor light source.....	50
2.4 Control (a), 1 (b), 5 (c) and 10 (d) % ^{w/w} fullerene coatings at 60x magnification....	51
2.5 Absorption spectra of the red and yellow cut-off filters.....	54
2.6 Surface temperature of coatings in isothermal photochemical chamber.....	56
2.7 Structures of oxidation by-product of Demeton-S.....	57
2.8 Percent reduction of Demeton-S on coatings in ambient air relative to coatings in a nitrogen purged atmosphere.....	65
4.1 Mass spectrum of Demeton-S.....	71

List of Abbreviations

$^1\Delta_g$ – singlet molecular oxygen
2-CEES – 2-chloroethyl ethyl sulfide
2-CEPS – 2-chloroethyl phenyl sulfide
 $^3\Sigma_g^-$ - triplet molecular oxygen
AChE – acetylcholinesterase
°C – degree Celsius
C₆₀ – 60 carbon buckminsterfullerene
 $^1C_{60}$ – singlet-state C₆₀
 $^3C_{60}$ – triplet-state C₆₀
CD – Cyclodextrin
CWA – Chemical Warfare Agent
cm – centimeter
CN – cyano group
CN⁻ – cyanide ion
ClCN – cyanogen chloride
DANC – decontaminating agent, non-corrosive
Dem – Demeton-S
DSC – differential scanning calorimetry
g – gram
GA – Tabun
GB – Sarin
GC/MS – Gas chromatography/mass spectroscopy
GD – Soman
HD – > 92 % distilled *bis*(2-chloroethyl) sulfide
HDI – hexamethylene diisocyanate
HOMO – highest occupied molecular orbital
ISC – intersystem crossing
lb – pound
kg – kilogram
LCt – lethal concentration time
LCt₅₀ – lethal concentration time to 50 % of population
LD – lethal dose
LD₅₀ – lethal dose to 50 % of population
LD_{LO} – lowest observed lethal dose
LSD – lysergic acid diethylamide
m – meter

m/z – mass to charge ratio
Mal – Malathion
MIL-PRF – military performance based specification
MIL-PRF-85285 – specific military polyurethane formulation identification
mg – milligram
mL – milliliter
mol – mole
OP – organophosphorous
POM – polyoxometalate
psi – pounds per square inch
ROS – reactive oxygen species
TCE – tetrachloroethane
 T_g – glass transition temperature
 μg – microgram
 μL – microliter
 μm – micrometer
UV – ultraviolet
Vis – visible
VX – *O*-Ethyl *S*-(2-diisopropylaminoethyl) methylphosphonothioate
 $^w/w$ – by weight
W – watt
WW I – World War I
WW II – World War II
 θ – contact angle
 γ_L – liquid-vapor interfacial tension
 γ_S – solid-vapor interfacial tension
 γ_{SL} – solid-liquid interfacial tension

Abstract

DEVELOPMENT AND ANALYSIS OF SELF-DECONTAMINATING COATINGS

Jeffrey G. Lundin

George Mason University, 2011

Thesis Director: Dr. Robert F. Cozzens

Chemical warfare agents (CWAs) are amongst the deadliest known chemicals. Despite international agreements which ban their use, threats posed by CWAs remain high, especially considering recent global events.^{1, 2} Although commonly referred to as poison gases, CWAs are most often liquids, which exhibit degradation half-lives on the order of days to several weeks, depending on conditions, classifying them as persistent threats.³ Therefore, following their dispersion, the most likely mode of exposure an individual will encounter is contact with residual agent on a contaminated surface. To reduce the risk, this research incorporated novel catalytic additives into commercial military urethane coatings, thereby imparting continuous self-decontamination to any paintable surface. An ideal self-decontaminating coating must quickly detoxify harmful surface residing chemical agents, maintain the integrity of the original surface and be cost effective. Novel organic and organometallic additives were designed, synthesized and incorporated into commercial resin systems at low loadings.

Additives selected for the investigation included fullerene, cyclodextrin, and polyoxometalate compounds. CWA simulants employed in the examination of surface reactivity included 2-chloroethyl ethyl sulfide, 2-chloroethyl phenyl sulfide, Demeton-S and Malathion. Upon illumination with visible light, the fullerene containing coatings exhibited photocatalytic degradation of CWA simulants on the surface, which resulted in oxidation by-products. Continuously active, catalytic self-decontaminating coating surfaces with activity against CWA simulants were developed and demonstrated without significant alterations to the coating's physical properties.

1. Background

1.1 Introduction

Surfaces contaminated with chemical warfare agents (CWAs) create substantial risks to rescue and emergency responders, equipment recovery personnel, medical staff and decontamination teams. Innocent civilians are susceptible to exposure months following a release if the area has not been properly and completely decontaminated.⁴ After the release of a chemical agent, a general precaution includes prohibiting reentry to the affected area until complete natural attenuation of the hazardous compound.⁵ However, this approach is not practical when dealing with an area of high public use, high economic importance, or concerning expensive and essential equipment, particularly of military value.

The decontamination processes commonly employed to rid the surfaces in affected areas and equipment of residual chemical agents have numerous shortcomings.³ Decontamination of an affected area requires specially trained personnel who must wear cumbersome safety attire to prevent exposure during the process. Furthermore, the decontamination solutions used are frequently caustic to individuals and corrosive to equipment. The fact that the decontamination solutions are corrosive prohibits their use on all aluminum substrates, such as aircraft, and consequently leaves no option other than to use household detergents and water. The utilization of post-exposure decontamination

solutions presupposes that an exposure event is known and has, in fact, been detected. A CWA release may be too small to be detected, yet a concentration sufficient to harm an individual may remain on the contaminated surface. The entire aforementioned procedure is extremely cumbersome, costly and time consuming.⁶

A chemical warfare agent is a compound designed specifically to most effectively incapacitate or kill targeted subjects.⁶ Chemical warfare agents are placed in one of six broad categories based on the symptomatic effects which the chemical agents inflict upon the exposed victim. The six broadly defined classes are: lacrimating agents, blood agents, pulmonary agents, incapacitating agents, vesicating agents and nerve agents. Several of the most notable CWAs are summarized in Table 1.1.⁶ The remainder of the background will primarily focus on the vesicants and nerve agents due to agent persistence; however, a very brief description of the other CWAs is also included.

Table 1.1: NATO codes for chemical agents.

Chemical Name	Common Name	NATO Code	CAS Registry
2-Chlorobenzal malononitrile (1)	Tear gas	CS	2698-41-1
Hydrogen cyanide (2)	Hydrogen cyanide Prussic acid	AC	74-90-8
Carbonyl chloride (3)	Phosgene	CG	75-44-5
3-Quinuclidinyl benzilate (4)	-	BZ	6581-06-2
Dichloro (2-chlorovinyl)arsine (5)	Lewisite	L	541-25-3
<i>Bis</i> (2-chloroethyl) sulfide (6)	Sulfur mustard Mustard gas LOST Yperite	H HD (distilled)	693-07-2
<i>O</i> -Ethyl <i>N,N</i> -dimethylphosphoramidocyanidate (7)	Tabun	GA	77-81-6
<i>O</i> -Isopropyl methylphosphonofluoridate (8)	Sarin	GB	107-44-8
<i>O</i> -Pinacolyl methylphosphonofluoridate (9)	Soman	GD	96-64-0
<i>O</i> -Ethyl <i>S</i> -(2-diisopropylaminoethyl) methylphosphonothioate (10)	VX	VX	50782-69-9
<i>O</i> -Isobutyl <i>S</i> -(<i>N,N</i> -diethylaminoethyl) methylphosphonothioate (11)	V-gas Soviet-VX	VR	159939-87-4

1.2 Terminology

Toxicities for most agents are well documented and are represented in several formats. The terms associated with each agent will be briefly defined to circumvent any confusion. Dose refers to the quantity of chemical received by the subject. A dose for toxicity research is often administered topically on the skin (dermal), injected directly into the bloodstream (intravenous), injected under the skin (subcutaneous), or swallowed (oral). The lethal dose (LD) which kills 50 % of a given population is abbreviated by

LD₅₀. Often LD₅₀ is normalized as a measurement of the mass of chemical (usually mg) per kilogram of body weight (mg·kg⁻¹). Lethal dose low (LD_{LO}) expresses the minimum quantity by mass of chemical agent per kilogram of body mass which has been observed to be fatal to an individual of a given population. The lethal concentration time (LCt), measured in milligram minutes per cubic meter (mg·min·m⁻³), is frequently used to measure the toxicity of exposure to the vapor or aerosol forms of a substance. This unit is purely the product of concentration (mg·m⁻³) and time (min). LCt is useful to determine the lethality of variable combinations of concentration and time.⁷ Correspondingly, LCt₅₀ signifies the lethal concentration time sufficient to kill 50 % of a given population. For example, a compound with an LCt₅₀ of 50 mg·min·m⁻³ is lethal to 50 % of the population that has received an exposure of 50 mg·m⁻³ for a duration of 1 min. The same compound is also lethal at a concentration of 5 mg·m⁻³ for 10 min.

1.3 CWA Classification

The first class of CWA to be discussed includes the lacrimating agents. Lacrimation is the production and shedding of tears; consequently, this class of CWA primarily affects the lacrimal glands, causing an uncontrollable flow of tears from the eyes, thus the common name referring to this type of agent is “Tear Gas.” Exposures to these agents induce ocular irritation and reduction of vision, and are capable of effectively incapacitating targets non-lethally. Chemical riot control agents consist largely of lacrimating agents.⁸ While the term “tear gas” can be broadly applied to the entire class of compounds, it is conventionally used to refer to the specific compound 2-

chlorobenzalmalononitrile (**1**), also known by the NATO code CS. The chemical structure of CS (**1**) is presented in Figure 1.1. CS is utilized by many police and peace keeping forces throughout the world. CS is generally considered a non-lethal agent, however when used in a closed air environment, increased concentrations can cause serious health complications and deaths have been attributed to its use.⁸ Additionally, CS is commonly incorporated in training regiments as a simulant for more harmful chemical agents to test the effectiveness of respirators.

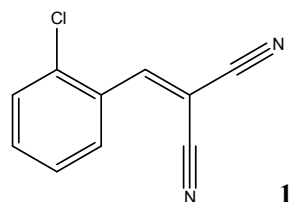


Figure 1.1: Structure of CS (**1**).

The most well-known members of the blood agent class consist of cyanide based compounds in which the cyano (CN) group is typically bound to a group I element such as H, Na, or K. The toxicity of cyano compounds results from the dissociation of the compound into the constituent alkali and cyanide ions (CN⁻). The cyanide ion binds to and inhibits the enzyme, cytochrome C oxidase, disrupting the respiration pathway and causing cytotoxic hypoxia.⁹⁻¹¹ Hydrogen cyanide (**2**) is commercially used in many industrial processes, largely in the production of nylon 6,6.¹¹ Hydrogen cyanide is the toxic component in the notorious compound Zyklon B, which was used in gas chambers

of concentration camps during World War II.¹² Zyklon B consisted of a mixture of stabilizers, adsorbents, hydrogen cyanide, and cyanogen chloride (ClCN).⁹ Despite their high toxicities, blood agents are non-persistent threats due to their extreme volatility. Consequently, the blood agents do not typically require decontamination efforts because they quickly evaporate into the air and diffuse to non-toxic concentrations.

Pulmonary agents disrupt the ability of the exposed victims to breathe.¹³ These agents cause excess excretion of fluid in the throat and lungs, thus increasing the difficulty to breathe as well as inducing coughing and choking.¹⁴⁻¹⁶ Other symptoms include vomiting, burning of the throat, pain in the chest and general respiratory failure.¹⁶ Chlorine gas (Cl₂) and phosgene (**3**), both widely used in World War I,¹⁷ are classified as pulmonary agents (Figure 1.2). Although pulmonary agents are very toxic,^{15, 16} there are numerous industrial uses for chlorine and phosgene. Consequently, pulmonary agents are not as strictly controlled as the more exclusive warfare agents. Furthermore, these agents are non-persistent and do not require surface decontamination because they are gaseous at room temperature.

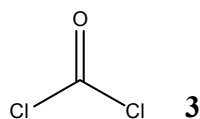


Figure 1.2: Structure of phosgene (**3**).

Incapacitating agents, another class of non-lethal agents, disable targets by inducing temporary psychological disruption.⁶ Various foreign militaries experimented

with mind altering agents following World War II, exploring the potential of psychotropic compounds as CWAs.¹⁸ Most agents were ultimately rejected and considered unsuitable for weapons. However, the incapacitating agent 3-quinuclidinyl benzilate (**4**), NATO code BZ (Figure 1.3), did reach military weaponization, but it was never put into operational use.¹⁸

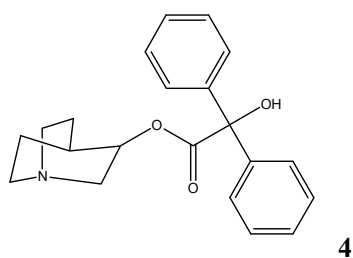


Figure 1.3: Structure of the incapacitating agent BZ (**4**).

1.4 Vesicants

Vesicant agents, along with nerve agents, pose the greatest threat of surface contamination. Vesicant agents cause serious blistering and chemical burn symptoms upon contact with skin, eyes and lung tissue.^{19, 20} There are two principle agents of this class, dichloro (2-chlorovinyl)arsine (**5**) and *bis*(2-chloroethyl) sulfide (**6**). Dichloro (2-chlorovinyl)arsine (**5**), often known by the common name Lewisite, was developed in the United States in 1918 (Figure 1.4).¹⁸ This compound is named after Winford Lee Lewis following his discovery of the thesis of Julius Arthur Nieuwland which detailed the synthesis of the compound.⁹ After initial integration into the U.S. military arsenal,

stockpiling of Lewisite was discontinued due to disadvantages in field persistence and long-term storage stability.

The vesicant that was highly stockpiled is *bis*(2-chloroethyl) sulfide (**6**). The name mustard is more commonly used to refer to *bis*(2-chloroethyl) sulfide (Figure 1.4) and originates from the pale yellow color and odor the compound exhibits which resembles the mustard plant. The yellow color and odor result from impurities present in the mixture when first produced by the Levinstein process.¹⁹ Pure *bis*(2-chloroethyl) sulfide (**6**) is actually colorless and odorless. The color of mustard agent can range, depending on purity, from clear to pale yellow and even black.¹⁹

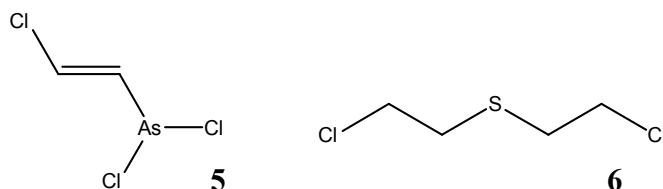


Figure 1.4: Structures of vesicants Lewisite (**5**) and HD (**6**).

There are several names which are used to refer to *bis*(2-chloroethyl) sulfide (**6**). The name Yperite is sometimes used to describe *bis*(2-chloroethyl) sulfide (**6**), which is a reference to its first military use on the battlefields of Ypres in World War I. LOST, the original German military name, was a result of the combination of the first two letters of Lommel and Steinkopf, the German General Staff members to first propose military incorporation of the chemical. NATO code has designated the capital letter “H” to

represent *bis*(2-chloroethyl) sulfide (**6**) and often is seen as HD, which corresponds to the distilled form of 92 % pure sulfur mustard. HD will be used in the remainder of this text for clarification.

HD was highly stockpiled because it is easily synthesized, stable during storage, persistent after release and very effective in causing casualties.²¹ As of 2009, there were 11,450 metric tons of HD were declared worldwide.²² Table 1.2 provides an overview of various physical properties of HD.

Table 1.2: Physical properties of HD (**6**).

Molecular Weight (g-mol ⁻¹)	159
Liquid Density (g-cm ⁻³ @ 20 °C)	1.27
Boiling Point (°C) (@750 mm Hg)	227
Melting Point (°C) (@750 mm Hg)	14.11
Vapor Pressure (mm Hg@20 °C)	7.2 x 10 ⁻²
Volatility (mg-m ⁻³ @ 20 °C)	610
Vapor Density (air = 1.0)	5.4
Solubility in Water (g-100 mL ⁻¹)	0.11

The blistering effect of HD is attributed to an alkylating mechanism.²³ Generally, a Cl⁻ is eliminated from one terminus, resulting in the formation of the carbocation sulfonium ion with the central heteroatom (sulfur), as depicted in Figure 1.5. The resulting sulfonium ion is very reactive towards a variety of nucleophiles and consequently reacts with the nucleotide guanine in DNA, effectively alkylating the

nucleotide. This action is particularly harmful to the skin, resulting in blisters and carcinogenic effects.^{20, 24-26}

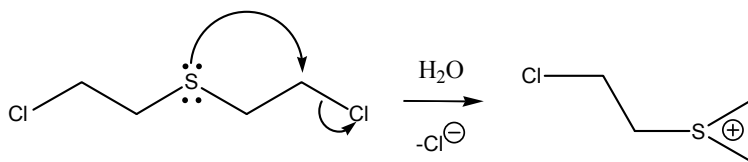


Figure 1.5: Formation of sulfonium ion from 6.

The concentration of HD required to induce vesication is extremely low and symptoms can appear at concentrations as low as 0.003 mg-m⁻³. However, the LD₅₀ of sulfur mustard, when applied to the skin, is 100 mg-kg⁻¹.⁶ The high lipophilicity of HD allows rapid penetration of the skin, at a rate of 1-4 μg-cm⁻²-min⁻¹.⁶ Symptoms, including severe blisters, begin to appear 12-24 hours following exposure.²⁷ This delay in presentation increases the danger of residual contamination due to a possible lapse in recognition of exposure to the agent and consequent inadequate decontamination. There is no specialized treatment following dermal exposure to vesicant agents. The skin is treated with antibiotics to prevent infection and soothing compounds to relieve painful symptoms as if it were a severe thermal or chemical burn.²⁸ Respiratory failure and systemic organ failure can result from excessive exposure of HD to lung and skin tissue. Historically, fatalities often occurred due to secondary infections of the massive blistering of the skin, especially prior to the invention of modern antibiotics.

1.5 Nerve Agents

The nerve agents are a class of CWA which comprise organophosphorous (OP) compounds that affect the nervous system. Specifically nerve agents, including OP pesticides, act to inhibit the enzyme acetylcholinesterase (AChE) in neurological synapses. In the muscarinic, nicotinic, and the central nervous systems, acetylcholine is an important neurotransmitter. Acetylcholine transfers a signal along the nerve pathway by leaving the axon and subsequently binding to a receptor. AChE facilitates the hydrolysis of acetylcholine into acetic acid and choline, which release from the receptor and reactivate the cholinergic receptors.²⁹ Release of the neurotransmitter from the receptor is essential to deactivate the nerve signal. Nerve agents inhibit AChE by irreversibly binding to the hydroxyl group of a serine in the active site of the enzyme.^{29, 30} The serine hydroxyl of AChE is phosphorylated by the nerve agent through the loss of a leaving group from the nerve agent as displayed in Figure 1.6.

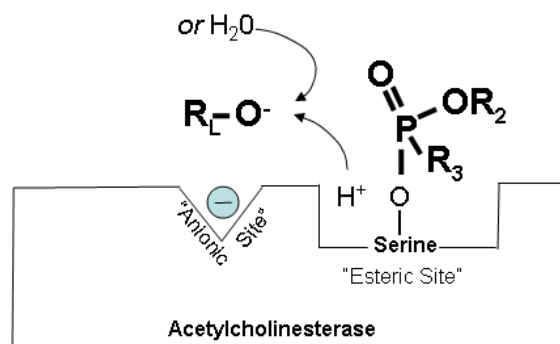


Figure 1.6: Phosphorylation of the active site of AChE by a nerve agent.³¹

The active site of AChE is inhibited by phosphorylation and AChE cannot catalyze acetylcholine. Therefore, an accumulation of acetylcholine occurs at the

receptor and causes overstimulation of the nervous pathway, which results in cholinergic toxic effects.²⁹ The muscarinic receptors almost exclusively use acetylcholine as the neurotransmitter to conduct signals and are therefore the most affected. Exposure to nerve agents initially present symptomatically as miosis, bronchoconstriction, salivation, lacrimation and loss of muscle control.⁶ Frequently, symptoms appear 2-18 hours following exposure.⁴

Another aspect concerning nerve agents is the permanent and irreversible binding to AChE. The amount of time required to irreversibly bind is referred to as aging. Aging is a result of the dealkylation of the bound agent, resulting in a very stable phosphorous-AChE bond.²⁹ The time required for aging to occur varies; the faster the agent ages the more rapidly treatment must be administered following exposure.³² Once aging has occurred, treatment has no effect and the only relief comes from the production of more AChE by the body, which can take several months if a lethal dose has not been administered. Treatment of nerve agent exposure focuses on the timely administration of a mixture of atropine and oxime solution, which stoichiometrically blocks further acetylcholine from binding to the receptor and allows the release and degradation of the nerve agent.⁶

Nerve agents can be divided into two subgroups consisting of the G-agents and the V-agents. The “G” in G-agents stands for either “German” or “Germany.” The “V” in V-agents does not necessarily represent a word, but has been designated to represent a series of particularly persistent agents. The G-agents were developed in Nazi Germany during the 1930’s and 1940’s.³³ The most important agents of this group are *O*-ethyl

N,N-dimethyl-phosphoramidocyanidate (Tabun) (7), isopropyl methyl-phosphonofluoridate (Sarin) (8) and pinacolyl methyl-phosphonofluoridate (Soman) (9), as seen in Figure 1.7. NATO has designated the G-agent chemicals Tabun, Sarin, and Soman with the code letters GA, GB, and GD, respectively. Sarin and Soman are similar in structure in that they are both methylphosphonofluoridate compounds, only exhibiting variation in the alkoxy substituent. Toxicities of the nerve agents are shown in Table 1.3.

Table 1.3: Toxicities of nerve agents.

Toxicity, administration	GA	GB	GD	VX
LD ₅₀ Rat, oral (μg·kg ⁻¹)	3700	550	NA	NA
LD ₅₀ Rat, subcutaneous (μg·kg ⁻¹)	193	103	75	12
LD _{Lo} Human, skin (mg·kg ⁻¹)	23	NA	18	0.086
LCt ₅₀ (mg·min·m ⁻³)	400	100	70	50
LD ₅₀ Human; skin ^a (mg) ⁶	1000	1700	50	10

^aLD₅₀ Human skin is calculated for a 170 lb male.

Of the G-agents, Sarin (8) and Soman (9) have been the most produced and stockpiled primarily due to their selection as agents of choice by the militaries of the United States and the former Soviet Union.²² The United States selected Sarin (8) for mass production into its chemical arsenal and currently holds a stockpile of thousands of tons.²² The former Soviet Union, which includes Russia and several Eastern European nations, stockpiled large amounts of both Sarin (8) and Soman (9) in its chemical arsenal, which is evident by the remaining declared stockpiles.²²

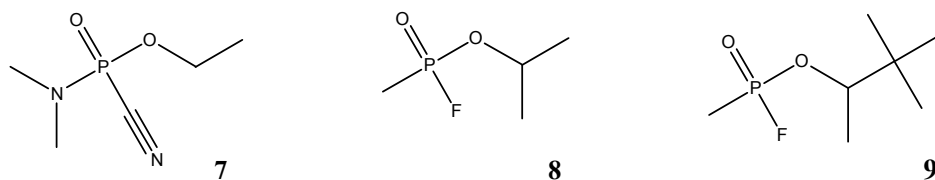


Figure 1.7: Structures of GA (7), GB (8), and GD (9).

However, G-agents are not considered persistent contaminants relative to HD and VX. At room temperature, Tabun (7) and Soman (9) exhibit hydrolysis half-lives of 8.5 and 5.25 hours, respectively. These half-lives are considerably short, especially in comparison to that of VX, which is 41 days.³ Also, while Sarin (8) exhibits a hydrolysis half-life which can range from 39 to 135 hours, a relatively high vapor pressure causes Sarin (8) to evaporate and quickly diffuse into the atmosphere to non-lethal concentrations leaving the surface free from contamination.³ Table 1.4 presents several physical properties of the G-agents.

V-agents are organophosphorous nerve agents, more specifically phosphonothioate nerve agents, first developed by British scientists in the 1950's.³³ V-agents are similar to G-agents in that they are organophosphorous compounds; however the primary difference is the thiolate sulfur bound to the phosphorous, which results in increased toxicity.

Table 1.4: Physical properties of GA (7), GB (8), and GD (9).

	GA – Tabun (7)	GB – Sarin (8)	GD – Soman (9)
Molecular weight (g-mol ⁻¹)	162	140	182
Liquid density (g-mL ⁻¹)	1.07 @ 25 °C	1.102 @ 20 °C	1.02 @ 25 °C
Freezing point (°C)	-50	-56	-42
Boiling point (°C) (@ 750 mm Hg)	247	147	167
Vapor pressure (mm Hg @ 25 °C)	7.0 x 10 ⁻²	2.9	0.4
Volatility (mg-m ⁻³ @ 25 °C)	610	17,000	3,900
Vapor density (air = 1.0)	5.63	4.86	6.33
Solubility in water (g agent/g water)	9.8/100 @ 25 °C	miscible	2.1/100 @ 20 °C

There are several V-agents, however *O*-ethyl *S*-(2-diisopropylaminoethyl) methylphosphonothioate (**10**), known as VX, is the most toxic and most important agent for research due its military importance. *O*-isobutyl *S*-(2-diethylaminoethyl) methylphosphonothioate (**11**), known by the NATO code VR, is the Soviet isomer of VX and is also of military significance. Structures of both VX and VR are shown in Figure 1.8. Because of its structural similarity, VR has a decontamination mechanism similar to VX. This research does not specifically focus on VR, as any work related to VX is believed to have a direct application to VR as well.

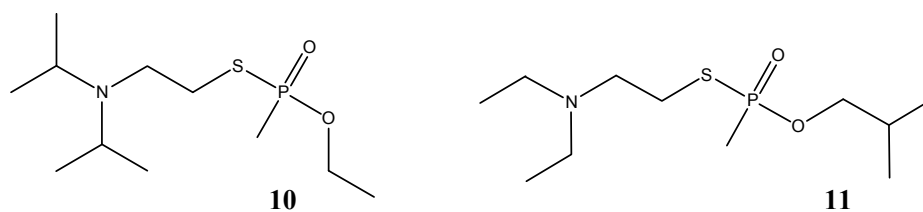


Figure 1.8: Structures of VX (**10**) and VR (**11**).

VX, in addition to Sarin (**10**), was selected by the United States military for mass production and stockpile.²² VX, an amber colored, tasteless, and odorless oily liquid, has a human dermal LD₅₀ of 0.040 mg·kg⁻¹ and an inhalation LCt₅₀ of 30 mg·min·m⁻³.⁴ Because the values of VX are much lower than those of G-agents, VX requires a far lesser dose to result in death. Table 1.5 presents several significant and pertinent physical properties of VX.

Table 1.5: Physical properties of VX (**10**).

Molecular weight (g·mol ⁻¹)	267
Liquid density (g·mL ⁻¹)	1.01 @ 25 °C
Melting point (°C)	-50
Boiling point (°C @ 750 mm Hg)	298
Vapor pressure (mm Hg @ 25 °C)	7.0 x 10 ⁻⁴
Volatility (mg·m ⁻³ @ 25 °C)	10
Vapor density (air = 1.0)	9.2
Solubility in water (25 °C)	30 g/100 g (miscible below 9.4 °C)

1.6 Historical use of CWA

Civilizations have resorted to the use of chemicals since the beginning of warfare. Early use occurred by burning materials with the aim to smoke out well entrenched defenders. Eventually, primitive chemical warfare developed into burning specific plants or materials such as sulfur containing compounds to increase effectiveness.¹⁸ Although the technology has improved, chemical warfare remains a viable method of combat today.

1.6.1 World War I

Use of the modern definition of chemical warfare began on April 22, 1915, on the Ypres battlefield during the Second Battle of Ypres of World War I.¹⁷ The German Army lined up canisters of chlorine gas and punctured the containers, which released a plume of yellow-green colored chlorine gas carried by the prevailing winds into the unsuspecting French Army. The French Army, after initially preparing for an attack from behind a smoke screen, quickly realized it was a poisonous gas attack and scrambled for retreat. Most notably, the battle at Ypres marked the beginning of the significant use of chemical weapons during WW I.³⁴

Within months of the initial attack, the French and British armies countered with their own chemical weapon development and attack. As WW I was waged, early respirators were developed and more effective delivery methods (such as gas filled artillery shells) were employed to reduce the reliance on favorable wind conditions. Phosgene was proven to more effectively evade the respirator defenses. Phosgene does

not induce as strong a coughing reflex as chlorine, therefore exposure goes unnoticed and does not quickly prompt donning of respirator gear. Often chlorine and phosgene were mixed together for use in a single shell.³⁴ Deaths from the use of chlorine and phosgene comprised a low percentage of the overall casualties; however, the possibility of chemical attacks at any time required either side to be constantly prepared with gas masks and also instilled a fear in soldiers comparable to no other weapon.

The effectiveness of the respirator led the Germans to incorporate sulfur mustard into their arsenal. Mustard was the first agent to present a persistent contact hazard and therefore necessitated decontamination protocols. Sulfur mustard was first synthesized in 1822 by M. Depretz, however the vesicant properties were not noted until 1860 by Frederick Guthrie.^{35, 36} In 1886, Viktor Meyer published a synthetic procedure for sulfur mustard which resulted in good yields and purity.³⁷ This method was eventually employed by the German military. On July 12, 1917, the German Army first employed mustard against the British Army at Ypres inflicting 15,000 casualties.⁹ The large number of casualties were caused as the soldiers donned their respirators and continued to fight, while their skin and eyes were unknowingly exposed to liquid and vaporized mustard. After 24 hours, many soldiers were found blind and covered with painful blisters. The first use of mustard was seen largely as a field test for the agent, which was viewed as a success and use subsequently accelerated.³⁴

Initially branded by the Germans as LOST, mustard was an effective agent at incapacitating enemy soldiers. Additionally, inhaled vapors of sulfur mustard in trenches caused a similar reaction in the throat and lungs. The lethality of mustard exposure

remained low; however painful blisters and health complications frequently resulted. A major disadvantage of mustard as an offensive weapon was its persistence in the soil for weeks after an attack, preventing the advancing army from safely occupying the abandoned objective. However, large amounts of mustard were deployed for defense by the German Army during its retreat in 1918. German production of mustard peaked at over 1,000 tons a month by 1918.³⁴ Germany had a far greater potential to produce chemical warfare agents than the allies due to its previously established chemical infrastructure that remained from its successful dye industry.

World War I saw both the introduction and pinnacle of the massive implementation of chemical warfare. The lasting painful effects, non-selective targeting, and potential to cause mass casualties created an international condemnation of chemical warfare. Despite unilateral disapproval covert chemical weapon development programs continued.³³

1.6.2 Nerve Agent Development

The synthesis of Tabun (7), by Gerhard Schrader of Germany, marked the development of the first G-agent. Schrader was performing pesticide research and noticed ill effects on both himself and his assistant. Nazi policy was to report all discoveries with military potential to the Ministry of War which began the search for even more potent nerve agent compounds. After the discovery of Tabun in 1936, Sarin (8) was discovered in 1937 and Soman (9) was developed by 1944.³³ High capacity industrial plants for Tabun and Sarin were constructed and began producing weapons

grade nerve gas during WW II. Nerve agents were never used due to a tremendous fear of retaliatory attack during WW II. Following the Allied march into Germany, Tabun and Sarin production plants were discovered and scientists divulged formulas to the conquering militaries.³³

The only documented CWA exposure by military personnel to chemical weapons in Europe during World War II occurred when the United States' ship SS John Harvey was attacked and sunk while unloading 100 tons of mustard weapons in port at Bari, Italy on December 2, 1943. The crew and dock workers suffered exposure to the agent, including 600 casualties and 83 fatalities.⁹ Additionally, the surrounding waters were contaminated with the agent as the sinking ship deposited its cargo on the bottom of the Mediterranean Sea. The agent persisted in the sea and has affected civilian fisherman and others who have worked on the sea for decades.

Following World War II, both the Western Allies and the Soviet Union acquired knowledge of the secret German chemical weapon operation. As cooperation between the victorious powers deteriorated, each began its own chemical weapons programs by assimilating the German developed G-agents into their arsenals and focused on the development of new nerve agents.³³

British chemical weapon research expanded upon pesticide work being performed in the 1940's and 1950's and created the highly toxic V-agents class of chemical weapons. The new agent, VX, was later adopted into the chemical arsenal of the United States in 1958. Concurrently, the Soviets developed an isomer of VX that exhibited comparable toxicity. This isomer is referred to Russian VX or VR.³³

Other chemical releases have been infrequent. In 1963, Egypt used mustard while intervening in Yemen.¹⁸ In 1968, a aerial spray tank leaked VX across thousands of acres near Dugway Proving Ground, Utah, and caused six thousand sheep casualties while more significantly igniting public outcry concerning the safety of the potent chemical agent.³³

The Iran-Iraq war, which lasted from 1980-1988, was host to an enormous amount of chemical weapon use. The Iraqi military campaign against Iran employed the use of sulfur mustard agent and Tabun.³⁸ The chemical weapons possessed by the Iraqi military were also used against civilians of both Iran and Iraq. Iranian citizens were attacked and terrorized by chemical attacks from Iraq. The Kurds of Iraq were attacked by their own national government in several acts of genocide utilizing the potent combinations of mustard and nerve agents.³⁹ The Halabja, Iraq chemical attack was the largest documented use of chemical weapons against civilians.³⁹ Furthermore, during the Persian Gulf War, the United States military was extremely concerned about chemical agent attack retaliation in response to the invasion of Iraq.

1.6.3 Terrorist Threat

More recently, two terrorist attacks which were carried out by the religious cult Aum Shinrikyo in Japan utilized chemical warfare agents. The first attack, which occurred on June 27, 1994, in the city of Matsumoto, included the release of the nerve agent Sarin across several sites of the Kaichi Heights area.² In this attack, seven people died and over two hundred were injured.² The second act by the same cult occurred on

March 20, 1995, in the Tokyo subway system.^{1, 40} Sarin was released at five sites throughout the Tokyo Metro.^{1, 40} The members conducting the act carried plastic bags filled with the nerve agent onto the subway system, penetrated the bags with sharpened umbrella tips and quickly evacuated.³³ Twelve people were killed in the attack, fifty-four people were seriously injured and thousands suffered minor effects.^{33, 40} The act was targeted at trains passing under or through the government district of Japan. The cult was also known to possess and use the nerve agent VX in some successful assassination attempts.⁴¹ In May of 1995, a burning bag containing hydrogen cyanide was found in the Japanese subway system, as well as several other non-ignited bags. The quantity of agent was estimated to be sufficient to kill 20,000 people, if not for the immediate action taken by security personnel.

The history of CWA use demonstrates several important points. First, CWAs have been employed around the world, with no area that is free from the threat. Second, repeatedly throughout history chemical weapons have been used despite international condemnation and treaties banning their use. Additionally, independent rogue organizations may now have access to these deadly chemicals. Finally, the potency and persistence of CWAs have increased dramatically. Furthermore, the decontamination process following CWA exposure has not kept pace with the development of evolving threats. The need for detection currently also demonstrates the necessity for new continuous decontamination approaches.

1.7 CWAs of Interest

HD and VX are the particular CWAs of interest concerning surface decontamination because both agents are incredibly persistent in the environment. Neither agent readily evaporates or hydrolyzes, especially compared to the G-agents. Large stockpiles of HD and VX are known to exist throughout the world. HD has been extensively stockpiled since WW I because of its effectiveness and simple synthesis. VX has been extensively stockpiled because it is the most potent of the nerve agents. From a chemical perspective, both HD and VX present the most difficult decontamination challenges, as they require strong reactants and also may produce toxic by-products.⁴²

1.8 Decontamination Solutions

Current decontamination processes utilize liquid solutions to chemically degrade the agent. Typically, an exposed surface is rinsed with the selected solution and scrubbed vigorously. Yet, successful decontamination solutions fall short in many aspects. They are often corrosive and caustic to the individual performing the decontamination as well as the asset being decontaminated.⁴³ Furthermore, the solution may merely wash away the contaminant and, if aqueous, result in large volumes of contaminated water.

The first military decontamination solutions used were bleaching powders developed by the allies in WW I, which consisted of a solution of calcium hypochlorite (Ca(OCl)_2). Additionally, Dakin's solution, composed of sodium hypochlorite and boric acid, was also employed; however the solution is unstable once mixed, requiring on-site preparation and immediate use.⁹ Current protocols recommend 0.5 % sodium or calcium

hypochlorite solutions for decontamination of the skin, while a 5 % concentration is recommended for equipment.⁶ However, equipment composed of aluminum, such as aircraft, are incompatible with hypochlorite solutions due an extreme susceptibility to corrosion. Numerous specialized decontaminating solutions have been developed throughout the years, however most fall short of being effective, non-corrosive and safe to use. This frequently results in the use of soap and water solutions, which do not degrade or detoxify the contaminants.

Decontaminating agent, noncorrosive (DANC), a commercially available product, is composed of a 1 to 15 ^{w/w} solution of the active chlorine compound dichlorodimethylhydantoin (RH 195) in tetrachloroethane (TCE). DANC is effective against HD and VX, but not G-agents. DANC functions through a reaction with H₂O, forming hypochlorous acid, which then reacts with the agent. DANC facilitates metal corrosion in the presence of moisture and frequently swells and damages polymeric materials, yet DANC is less corrosive than bleaches, while acting faster and possessing superior solubility properties than concentrated hypochlorite solutions. Serious toxicity from inhalation and absorption of DANC through the skin resulted in its discontinuation and it was subsequently discarded by the Navy following World War II.⁴⁴

Decontamination Solution 2 (DS2) was developed in 1951 and incorporated into military protocol in 1960. DS2 is a general purpose, ready to use decontaminant. DS2 also offers long term storage stability and a large temperature range of activity (-26 to 52 °C).⁴² The chemical composition of DS2 is diethylenetriamine (70 % ^{w/w}), ethylene glycol monomethyl ether (28 %), and sodium hydroxide (2 %).⁴² The active component

in this solution was found to be the conjugate base of the ethylene glycol monomethyl ether, which works well with both mustard and V-agents at ambient temperatures. A major drawback of DS2 is that it frequently damages polymer based surfaces such as paints, plastics, rubber, and leather. Because of this, application time is limited to 30 min on such surfaces.⁴² DS2 is also harmful upon contact with skin as well as inhalation. When being applied to an affected surface, the individual needs to wear full respirator, eye shield, and chemical resistant gloves to protect oneself from the decontaminating solution. Additionally, a reaction product resulting from DS2 use was found to cause birth defects in rats.⁴² The final disadvantage with DS2 is that it rapidly degrades and loses its potency upon contact with air and large amounts of water.⁴² Reactions with the atmosphere slowly degrade the decontaminating ability of DS2. These reactions include: the reaction of carbon dioxide with the sodium hydroxide to form sodium carbonate; reaction of carbon dioxide with the amine in DETA to form solid amine carbonate; and the absorption of water.⁴⁴ For these reasons and others, DS2 was also discontinued.

Scientists at Sandia National Laboratory developed an aqueous decontaminating foam called DF-200. Initially DF-100 was developed in 1999, however DF-200 improved upon DF-100 through pH optimization and a faster reaction rate with HD. DF-200 has shown to completely eliminate GD in 1 minute, VX in 15 minutes, and HD in 15 minutes, in addition to being environmentally benign. DF-200 was developed with the primary objective of decontaminating civilian facilities in the event of a domestic terrorist attack in urban environments,⁴⁵ however logistically, this solution is not very practical as it requires foam spraying equipment.

Decon Green Classic is another commercial product that exhibits extraordinary decontamination ability. Decon Green is a solution based decontaminant; however, the decontaminant has deleterious effects upon coatings and plastics, such as the ocular in a gas mask. New Decon Green was developed to remedy the reactivity of the decontamination solution with coatings and polymers. New Decon Green succeeds in reducing the amount of damage caused to such surfaces; however the decontamination ability is sacrificed.⁴⁶⁻⁴⁹

A common problem among all decontamination solutions was decontamination of agent that is sorbed into a coating.⁵⁰⁻⁵³ The applied solution works only on the exposed agent with which it is available to chemically contact and react.

1.9 CWA Simulants

Because it is impractical to work with real chemical warfare agents in a research environment, CWA decontamination research typically incorporates less harmful substances with which to mimic and simulate the incredibly toxic CWA.⁵⁴ These compounds, which share similar chemical and physical properties with CWA, but also exhibit reduced toxicity, are referred to as simulants. There are several criteria which must be considered prior to selection of such compounds. First, the simulant compound must exhibit similar stereochemical interactions, acid-base relationships, and reduction-oxidation potential as the CWA. The second criterion is that the simulant must exhibit similar physical properties, the most important of which are vapor pressure and polarity. These most significantly affect interactions of the simulants with surfaces. Finally and

most importantly, the simulant must be much less toxic than the CWA. CWAs are incredibly potent and dangerous, therefore the toxicity of the simulants must be minimal in order to create a safe and practical laboratory working environment.^{4, 55}

There are numerous compounds which are similar in chemical structure to HD. The most important functional group which must be present in an effective HD simulant is the $\text{RSCH}_2\text{CH}_2\text{Cl}$ moiety. The terminal Cl affects reactivity of the sulfide center, which is the target of oxidation. The sulfur in HD is less reactive towards both hydrolysis and oxidation than a sulfur in alkyl sulfides due to the electron withdrawing effects of the terminal chlorines.⁵⁶ It has been mutually agreed upon in the literature that no single simulant is sufficient to cover all aspects of decontamination and consequently, as in other studies, this research utilizes two simulants for HD, 2-chloroethyl ethyl sulfide (2-CEES) (**12**) and 2-chloroethyl phenyl sulfide (2-CEPS) (**13**), as depicted in Figure 1.9.



Figure 1.9: Structures of HD simulants 2-chloroethyl ethyl sulfide (**12**) and 2-chloroethyl phenyl sulfide (**13**).

2-CEES is structurally very similar to HD and offers similar chemical reactivity, yet exhibits a higher vapor pressure.⁵⁴ 2-CEPS contains a bulky phenyl group, which affects the steric interactions and reactivity of the central sulfur relative to HD. However,

the vapor pressure and persistence of 2-CEPS are closely related to those of HD.⁵⁷ The non-bonding electron pair of the central sulfur in 2-CEPS is stabilized via conjugation to the adjacent aromatic phenyl group. Numerous other groups have successfully utilized these compounds as simulants for research in decontamination methods of HD.^{46, 57-65} Several of the important physical properties of HD and the simulants are compared in Table 1.6.

Table 1.6: Physical properties of HD compared with simulants.

	HD (7)	2-CEES (12)	2-CEPS (13)
Molecular Weight (g-mol ⁻¹)	159	125	173
Liquid Density (g-cm ⁻³ @ 20 °C)	1.27	1.07	1.17
Boiling Point (°C) (@ 750 mm Hg)	227	156	246
Vapor Pressure (mm Hg @ 20 °C)	7.2 x 10 ⁻²	3.79	1.86 x 10 ⁻²

Additionally, there are numerous compounds capable of simulating VX (10) in a laboratory environment. The most important aspects of VX simulants are reduced toxicity and the presence of the phosphonothioate moiety. This region is the target for effective destruction of VX (i.e. oxidation) and therefore needs to be included in the simulant molecules.⁴² Additional properties which need to be considered are vapor pressure, persistency and polarity. Taking into account all of the requirements for an appropriate simulant, Demeton-S (Dem) and Malathion (Mal) were selected. These simulants are known commercial pesticides, which is consistent, as this class of CWAs was derived from pesticides. Figure 1.10 presents the chemical structures of VX and selected simulants. Dem and Mal are both commercial pesticides which previous

research efforts have utilized as simulants for VX.⁶⁶ Dem shares a similarity to VX in that it has a central phosphorous bound to a divalent sulfur, an ethoxy group, and a double bond to an oxygen atom. Dem is an excellent simulant because the relative reactivity of the P-O bonds and the P-S bonds can be observed through GC/MS product analysis. Furthermore, degradation pathways and the resulting products of Dem degradation have been identified by previous research.⁶⁷ Additionally, the *S*-alkyl group is of similar size to the *S*-alkyl bound group in VX, affording similar leaving potential. In addition, the *O*-ethyl groups are comparable to the *O*-ethyl group bound to the central phosphorous in VX. The combination of these factors leads to a simulant selection which can effectively mimic the target bonds. Mal exhibits a similar vapor pressure as VX,⁵⁴ has minimal toxicity and is commonly applied for insect control.⁶⁸

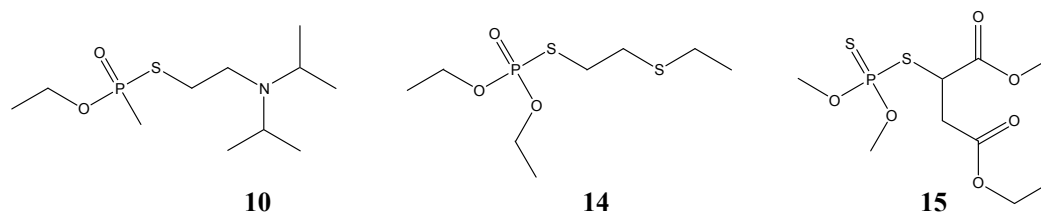


Figure 1.10: Structures of VX (**10**), Demeton-*S* (**14**) and Malathion (**15**).

1.10 Polyurethane Coatings

An immense range of polymeric coatings can be applied to virtually any surface. This research requires that the selected coating exhibit specific physical properties such as: ability to withstand physical stress (scratching, puncture, cracking), resistance to

most chemical solvents, affordability, ability to withstand a wide range in temperatures, and the ability to adhere to aluminum and steel. Polyurethane coatings, specifically the military polyurethane coating MIL-PRF-85285, fulfill all of the aforementioned requirements. MIL-PRF-85285 has met all standards set forth by the U.S. military and is consequently well-suited for this study. MIL-PRF-85285 is typically applied as a top coat to Air Force and Navy fixed wing aircraft. MIL-PRF-85285 is a two component high solids solvent borne polyester based urethane, which consists of a hydroxyl terminated aliphatic polyester cross-linked with an aliphatic hexamethylene diisocyanate (HDI) based polyisocyanate. Most importantly, this polyurethane coating should offer compatibility with a variety of additive chemistries that will be employed within.

1.11 Recent Research in Novel Reactive Systems

Recent research has been conducted in relation to the development and incorporation of novel reactive additives into various coating formulations in attempts to create functionalized coatings. Recent work with reactive coating additives include nonionic biocides,⁶⁹ quaternary ammonium biocides,^{70, 71} surface concentrating biocides,⁷² functionalized coatings,^{73, 74} and antimicrobial peptides.⁷⁵ Additionally, polystyrene adhesives containing modified fullerenes have exhibited singlet oxygen generation.⁷⁶ Although the innovative functional coatings are effective, none demonstrate activity against CWAs.

1.12 Selection of Reactive Coating Additives

The approach to utilize additives into coatings to create self-decontaminating reactive surfaces affords several benefits over creating new polymer coatings. Utilizing additives to impart surface reactivity is beneficial because they can be incorporated into a broad range of specialized coatings and also the established protocols to apply the coatings can be retained. However, there are also concerns associated with the selection of the appropriate additives.

C₆₀ fullerene has been documented to exhibit intriguing photochemical properties in solutions, which hold potential for development of a self-decontaminating coating.⁷⁷⁻⁸⁰ C₆₀ fullerene absorbs light throughout the visible spectrum as displayed in Figure 1.11. The sharp absorption peak at 400-425 nm is due to the absorption of solvent benzene. Moreover, exposure of C₆₀ fullerene in solution to visible light is known to result in excitation to a higher electronic state.^{77, 81, 82} Photosensitized fullerene exhibits the potential to transfer energy to nearby available molecular oxygen and create reactive oxygen species (ROS).^{78, 83, 84}

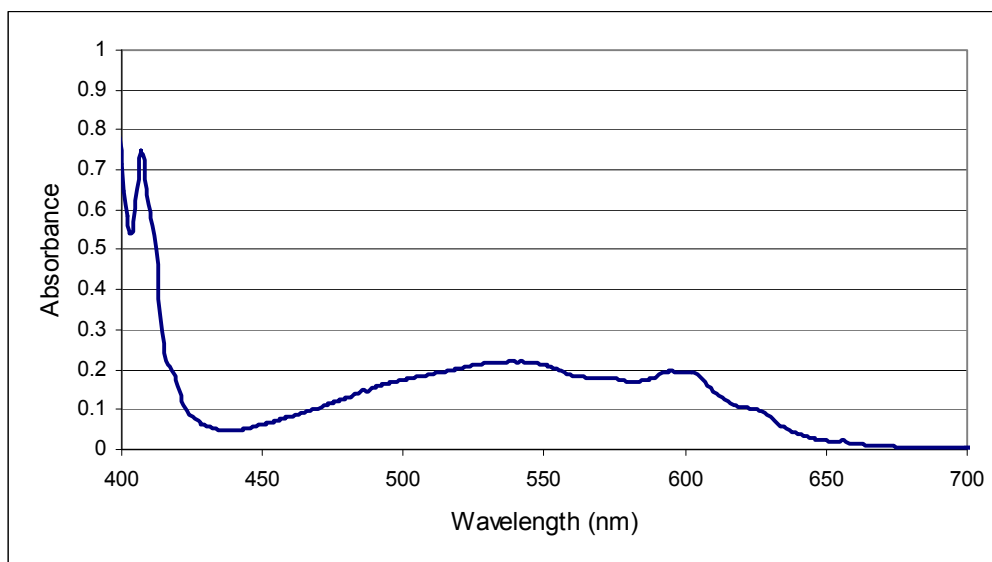


Figure 1.11: Absorption spectrum of fullerene in benzene.

Singlet and triplet states refer to the electrons in the highest occupied molecular orbital (HOMO) of a chemical bond. Each electron exhibits a spin that can have a sign of $\frac{1}{2}$ or $-\frac{1}{2}$. A singlet state refers to an electronic state of the HOMO containing a pair of electrons with anti-parallel spin which occupy a single molecular orbital. Therefore, the anti-parallel spins with signs of $\frac{1}{2}$ and $-\frac{1}{2}$ create a total sign of 0, which is referred to as a singlet. A triplet state occurs when two HOMO electrons occupy separate molecular orbitals and can each spin in either a positive or negative direction. Therefore, the three possible spin combinations which result for the bond are 1, 0, and -1, thus a triplet.

Upon exposure to visible light, C_{60} fullerene is first excited to its singlet state C_{60} ($^1C_{60}$). $^1C_{60}$ forms the triplet state species of C_{60} ($^3C_{60}$) via intersystem crossing (ISC). $^3C_{60}$ has a lifetime on the order of several μs , whereas $^1C_{60}$ has a lifetime of several

ns.^{77,85-87} This triplet state species of fullerene has the ability to convert ground state triplet oxygen ($^3\Sigma_g^-$) into singlet oxygen ($^1\Delta_g$), a ROS.^{78, 83}

The combination of high quantum yield and low rate of degradation by ROS make C₆₀ fullerene attractive as a photoactive coating additive.^{77, 78} Extensive studies have been conducted to analyze and characterize the photosensitivity of C₆₀ in solution with varying degrees of success.^{83, 85, 88-92} A novel antiviral system has been successfully developed with the incorporation of fullerene as a solid-phase photosensitizer into biological fluid.⁹³ Similarly, various photosensitizers have been shown to exhibit antimicrobial activity when incorporated into polyurethane coating systems under specific conditions.⁹⁴⁻⁹⁶ Recently, C₆₀ fullerene modified with intercalated constituents have displayed remarkable ability to produce singlet oxygen as well as exhibit antimicrobial activity in polymeric adhesive films.⁷⁶ Additionally, recent research has documented the photocatalytic ability of a C₆₀ fullerene species that is tethered to polymer beads and silica gel.^{97, 98}

Cyclodextrins (CDs) are molecules with the shape of 3-dimensional truncated cones, as displayed in Figure 1.12, and the radii of which depend on the number of repeating units in the cyclodextrin.^{99, 100} The repeating units in cyclodextrins consist of glucose which are connected to one another through α -1,4 glycosidic linkages.¹⁰¹ The most common forms of these molecules are the α -, β -, and γ -cyclodextrins, which correspond to 6, 7, and 8 membered rings, respectively.

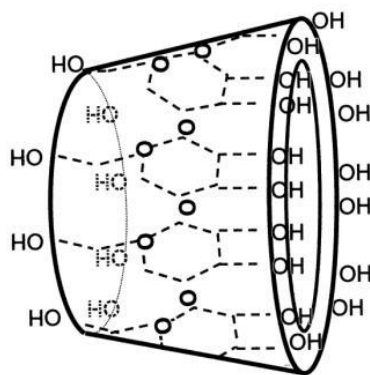


Figure 1.12: Truncated cone shape of cyclodextrin.

The general structure of cyclodextrins is shown in Figure 1.13. In addition to the unique ring structure, cyclodextrins can be further modified with the addition of reactive moieties designed to react with esters and thioethers (i.e. nerve and mustard agents). The molecule may act similar to a funnel in which the targeted agent fits and is oriented towards the reactive components for degradation. The cyclodextrins examined in this work are modified with transition metal elements such as iron (Fe) and nickel (Ni) to increase reactivity. The measure of the diameter of the CD is suspected to play an important role in its reactivity toward CWAs. The inner diameter at the wider opening of the cone for the non-metallated α -, β -, and γ -species are 0.57, 0.78, and 0.95 nm, respectively.^{101, 102} Host/guest interactions of the CD and target are dependent on both the diameter and the polarity/charge within the cavity of the CD. The interior of the funnel consists of non-polar C-C bonds while the exterior consists of the polar C-O region. Therefore, in aqueous solutions, the interior of the CD cone can be expected to exhibit preferential affinity towards HD and VX, both of which are hydrophobic.

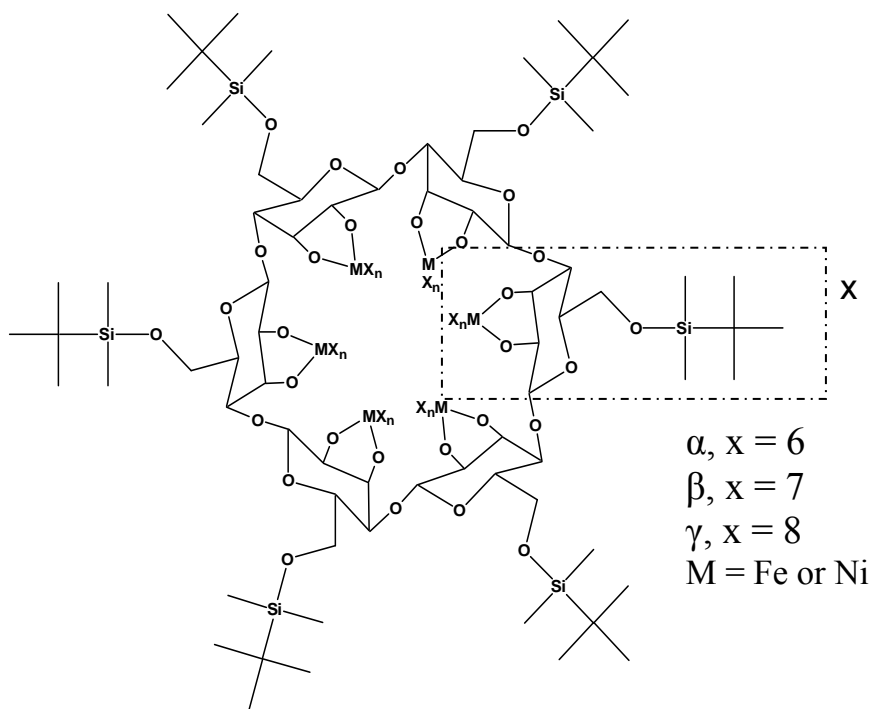


Figure 1.13: General structure of cyclodextrin (CD) additives.

Polyoxometalates (POMs) are another class of compounds consisting of assemblies of clustered metal (V, Mo, or W) oxides. POMs are the conjugate anions of heteropoly acids and have been a topic of interest for more than a century.¹⁰³ These molecules exhibit a variety of unique properties including a range of acidities, polarities, and redox potentials.^{104, 105} Such properties suggest that POMs can potentially be applied as effective oxidative catalytic coating additives. Individual POMs exist as one of several structure types, each of which results from the stoichiometric ratios of elements in the chemical formula and the possible conformations of the resultant edge sharing MO_6 octahedra. The POMs used in this work demonstrate one of two main structure types, the

Keggin structure and the Dawson structure. The Keggin structure consists of polyoxoanions with the general formula $\text{XM}_{12}\text{O}_{40}^{n-}$.¹⁰⁶ The Dawson structure describes polyoxoanions with the general formula $\text{X}_2\text{M}_{18}\text{O}_{62}^{n-}$.¹⁰³ In these formulas, X is most commonly a pnictogen (P, As, Si) or B; M is usually Mo or W, and n is the charge resulting from the valence of X . A counterion often accompanies the POM anion equal to the value n . Additionally, POMs have been documented to exhibit photoactivity, which presents a promising avenue to investigate the application of additive photocatalyzed surface decontamination.¹⁰⁷ Additionally, polyoxometalates containing tungsten incorporated onto porous silica have demonstrated unique photocatalytic behavior.¹⁰⁸

2. Results and Discussion

The objective of this research is to create a continuously active self-decontaminating surface. A continuously active, self-decontaminating coating system alleviates the necessity of contaminant detection and subsequent time consuming surface washing and scrubbing. An advantage to this reactive coating system is that inaccessible surfaces should automatically detoxify as well. This work aims to create such surfaces by incorporating select additives into a commercially available polyurethane coating formulation. Low percent additive loading (concentration) should allow the commercial polyurethane to retain its inherent desirable physical properties while incorporating detoxifying functionality. If the additives exhibit photochemical properties in solution, then these similar properties shall be examined when the additives are incorporated into coatings. The effects of varying the ambient conditions on the reactivity of the coatings and the resulting by-products are examined. From analysis of coating reactivity and by-product formation, mechanistic insight should be elucidated explaining observed results.

2.1 Overview of Experimental Approach

Although extensive studies have been conducted utilizing fullerenes, CDs, and POMs to determine their unique properties and relative reactivities in various solutions, little to no work has been done in the way of direct incorporation into a coating system.

It can be presumed that the activity of an additive may be significantly reduced due to encapsulation into the polymeric matrix; however, if this limitation is overcome, significant activity should remain at the coating-air interface. If successful, the expectation is that the additive in the coating should demonstrate behavior similar to that observed in neat or solution-based reactions and subsequently react with any contamination that may be on the surface. Upon exposure to hazardous analytes, such as pesticides or CWAs, the action of the additive in the coating would reduce the hazard and subsequently present a surface free from contamination.

Numerous neat additives were previously screened and the most active were selected for incorporation into MIL-PRF-85285 for surface property analysis. The initial evaluation to determine whether the additives adversely affected the performance characteristics of the coating included surface energy analysis and glass transition temperature (T_g) analysis. Further investigations included determining CWA simulant degradation capability of the coatings under various environmental conditions, such as exposure to regions of the visible light spectrum, temperature and time. For each condition, the surface by-products of the reactions were detected and identified to facilitate mechanism elucidation.

2.2 Down-selection

Coatings of 1, 5 and 10 % w/w fullerene additives were formulated for evaluation. The fullerene additives were observed to aggregate at concentrations greater than one percent, which reduces the dispersion and reactivity at the coating surface. The 1 % w/w

concentration was selected because of the minimal effect on the inherent properties of the polymer coating as compared to those at higher loadings, as well as the ability to impart significant surface reactivity. Therefore, the CD and POM additives were loaded into MIL-PRF-85285 at 1 % ^{w/w} for subsequent analysis in an effort to avoid potential aggregation of additives and adverse physical effects on the coatings. The CDs and POMs in this work were synthesized by collaborators at the University of Alaska Fairbanks, following published procedures.¹⁰⁹⁻¹¹¹ The series of coatings prepared with the additives is listed below in Table 2.1. The reference numbers given will hereafter be used to refer to each corresponding additive.

Table 2.1: Chemical formulas of the additives screened.

Ref #	Class	Molecular Formula	% ^{w/w}
Fullerene	Fullerene	C ₆₀	1,5 & 10
α-Fe	CD	Fe ₆ C ₇₂ H ₁₃₂ O ₃₀ Si ₆	1
β-Fe	CD	Fe ₇ C ₈₄ H ₁₅₄ O ₃₅ Si ₇	1
γ-Fe	CD	Fe ₈ C ₉₆ H ₁₇₆ O ₄₀ Si ₈	1
α-Ni	CD	Ni ₆ C ₇₂ H ₁₃₂ O ₃₀ Si ₆	1
β-Ni	CD	Ni ₇ C ₈₄ H ₁₅₄ O ₃₅ Si ₇	1
γ-Ni	CD	Ni ₈ C ₉₆ H ₁₇₆ O ₄₀ Si ₈	1
P1	POM	α ₂ -K ₈ P ₂ W ₁₇ O ₆₁ (Co ²⁺ ·OH ₂)·16H ₂ O	1
P2	POM	α ₂ -K ₇ P ₂ W ₁₇ O ₆₁ (Fe ³⁺ ·OH ₂)·8H ₂ O	1
P3	POM	α ₂ -K ₈ P ₂ W ₁₇ O ₆₁ (Ni ²⁺ ·OH ₂)·17H ₂ O	1
P4	POM	α ₂ -[(n-C ₄ H ₉) ₄ N] ₉ P ₂ W ₁₇ O ₆₁ (Ni ²⁺ ·Br)	1
P5	POM	α/β-K ₆ P ₂ W ₁₈ O ₆₂ ·10H ₂ O	1
P6	POM	[Fe ^{II} (bpy) ₃][PW ₁₁ O ₃₉ Fe ₂ ^{III} (OH)(bpy) ₂]·12H ₂ O ^a	1
P7	POM	(Hdmbpy) ₂ [Fe ^{II} (dmbpy) ₃] ₂ [(PW ₁₁ O ₃₉) ₂ Fe ₄ ^{III} O ₂ (dmbpy) ₄]·14H ₂ O ^b	1
P8	POM	[N(CH ₃) ₄] ₁₀ [(PW ₁₁ O ₃₉) ₂ Fe ₂ ^{III} O]·12H ₂ O	1
P9	POM	Ti ₁₁ O ₁₃ (OPr ⁱ) ₁₈ ^c	1

^abpy = 2,2'-bipyridine; ^bdmbpy = 4,4'-dimethyl-2,2'-bipyridine; ^cPrⁱ = isopropyl

2.3 Coating Characterization

It is important that the physical properties of the coatings be maintained following the incorporation of the additives in order that the performance of the final coating conforms to the MIL-PRF specifications. The physical characterization of the coating, particularly the determination of surface energy and glass transition temperature, allows confident approximations of how well the additive containing coatings maintain performance.

2.3.1 Contact Angle Analysis

While several methods have been developed to measure the surface free energy of a coating, contact angle analysis has emerged to be the best method suited for this study. Additionally, contact angle measurements are regarded as the standard method for measuring surface free energy.¹¹² Contact angle refers to the angle which forms at the 3-phase boundary of the bottom edge of liquid when placed on a solid in a gaseous atmosphere. The angle is created by drawing a line tangent to the surface of the liquid at the point where the liquid and solid come in contact, such as in Figure 2.1. By measuring the contact angles of multiple liquids, each of which has a known surface tension, the surface tension of the solid surface can be determined by mathematical extrapolation.

In this study, measurements were performed using a video contact angle (VCA) instrument which consists of a syringe, a stage and a camera oriented orthogonally to the liquid drop and in the plane of the solid surface.

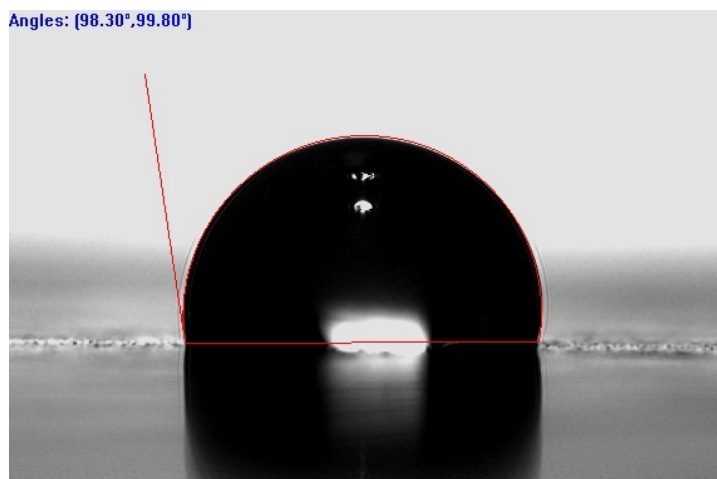


Figure 2.1: Image of a contact angle measurement.

Contact angle and surface energy analysis are critically important to the characterization of self-decontaminating coatings for several reasons. First, the incorporation of functional additives can affect surface energy which may offer insight into the surface segregation of the additive. A large change in surface energy suggests that not only has the polymer been altered, but the additive likely exists at the coating-air interface. The direction of the change, whether the surface becomes more or less polar, may also suggest the specific portion of the additive molecule that is exposed at the surface. Surface energy analyses provide insight as to how a liquid will spread and wet the surface, such as in the case of CWA. CWAs each have specific surface energies and the degree to which a CWA will spread (wet) can be predicted based on surface energy analysis. The greater the extent of spreading by the simulant on the surface, the higher the overall contact with the active coating surface, and therefore an increase in catalytic breakdown is expected. However, the disadvantage to greater affinity of CWA to a surface is a subsequent increase in the difficulty to wash or rinse the surface free of

contamination. The overall goal is to incorporate additives into the coating to impart surface reactivity while maintaining physical characteristics, specifically contact angle.

Several methods exist to calculate the surface free energy of a solid from liquid contact angle measurements. Of these, the Zisman plot method is the simplest and most convenient to simply compare solid surfaces.¹¹³ Zisman found that the plot of the cosine of the contact angle of a series of liquids versus the liquids' surface tensions resulted in a straight line. Zisman described the intersection of the straight line with a line at $y=1$ as the critical surface energy of the solid. The numerical value of the Zisman critical surface energy is not necessarily the actual surface free energy of the solid; however, it does provide relative values for comparison.

A more precise approach to measure the free surface energy of polymers was developed by Owens and Wendt,¹¹⁴ which is an application of Young's equation (equation 1).¹¹⁵ Young's equation relates contact angle of a liquid on a solid (θ) to the liquid-vapor surface tension (γ_L), solid-vapor surface tension (γ_S), and the solid-liquid surface tension (γ_{SL}).

$$\gamma_S = \gamma_{SL} + \gamma_L \cos\theta \quad (\text{equation 1})$$

The Owens-Wendt method is based on the assumption that there are two types of interactions which contribute to the surface free energy of solids, polar and dispersive forces. Therefore, the polar and dispersive parameters are required for the probe liquids, and each parameter will be calculated for the solid surface from the contact angles of the

probe liquids on the surface. The surface free energy is the sum of the energy of the two interactions. Table 2.2 includes the contact angles of three probe liquids (water, diiodomethane (CH_2I_2), and *n*-hexadecane ($n\text{-C}_{16}\text{H}_{34}$)), as well as the surface energies calculated using both the Zisman and Owens-Wendt methods for all coatings prepared in this study.

Table 2.2: Contact angles and calculated surface energies of various coatings.

Surface	Contact Angle (°)			Surface Free Energy (dynes/cm)				
				Zisman	Owens-Wendt			Δ control
	Water	CH_2I_2	$\text{C}_{16}\text{H}_{34}$	Surface	γ - dispers	γ - hydrog	γ - solid	
Control	88.06	64.43	27.69	21.1	26.0	3.7	29.7	0.0
C ₆₀ 1 %	101.48	61.39	32.09	23.2	27.8	0.4	28.2	-1.6
C ₆₀ 5 %	101.04	60.36	36.51	21.5	28.4	0.4	28.8	-1.0
C ₆₀ 10 %	100.63	64.68	24.88	24.7	25.9	0.7	26.6	-3.2
P1	93.12	74.02	47.47	6.9	20.7	3.4	24.1	-5.7
P2	91.97	75.52	47.35	5.7	19.9	4.0	23.9	-5.9
P3	90.78	78.40	44.78	6.6	18.3	5.0	23.3	-6.5
P4	93.13	74.97	49.22	4.7	20.1	3.6	23.7	-6.1
P5	90.43	73.48	40.78	11.6	21.0	4.3	25.3	-4.6
P6	90.28	72.02	43.15	9.9	21.8	4.1	25.9	-3.9
P7	90.30	71.33	45.22	8.2	22.1	4.0	26.1	-3.7
P8	93.65	72.83	46.93	8.1	21.3	3.1	24.4	-5.4
P9	98.13	77.05	45.22	10.9	19.0	2.3	21.3	-8.4
α - Fe	83.15	61.45	39.63	12.4	27.7	5.1	32.8	3.1
β - Fe	95.25	62.22	40.52	17.2	27.3	1.5	28.8	-1.0
γ - Fe	84.13	59.55	41.67	11.7	28.8	4.4	33.2	3.5
α - Ni	87.25	59.65	36.70	17.3	28.8	3.4	32.2	2.4
β - Ni	84.65	63.73	38.45	13.5	26.4	4.9	31.3	1.6
γ - Ni	86.30	67.73	38.68	12.9	24.2	4.9	29.1	-0.7

The surface energy of the coating affects the degree liquids will spread on the surface, which is defined in the specifications for an acceptable coating. The coating system being employed in this study, MIL-PRF-85285, has been specifically developed for aircraft which require water and liquids to bead off the surface. However, a self-

decontaminating coating requires that contaminant liquid contact with the surface is maximized. Therefore, the most successful additives are those which least affect surface energy as a lower surface energy would increase water and agent run-off, yet reduce decontamination. Conversely, a higher surface energy would result in decreased water beading, yet potentially greater surface decontamination capability due to agent spreading increasing the contact of the agent with the reactive surface.

In comparison of the surface energies calculated by the different methods, the Zisman critical surface energies were found to be universally lower than those calculated using the Owens-Wendt method. The Owens-Wendt method considers both the polar and dispersive interactions of a surface. Fullerene incorporation into the coating slightly increases the dispersive energy while greatly lowering the polar energy of the coatings. This combination results in slightly lower total surface energies of the coatings as compared with the control. All coatings containing POM additives resulted in lower Owens-Wendt surface energies than the control surface. Conversely, the coatings containing CD additives increased or only slightly decreased the surface energy with respect to that of the control. In fact, the only coatings which exhibited increased surface energies compared with the control contained CD additives. Overall, the majority of the coatings displayed surface energies within ± 6 dynes/cm of the control, which is in the range specified for a coating. In summary, the incorporation of the various additives at low loading concentrations, with exception of **P9**, did not adversely affect the surface energy of the resulting coating systems.

2.3.2 Differential Scanning Calorimetry

Differential scanning calorimetry (DSC) is a thermal analytical technique often used to characterize polymers by measuring the differential heat capacity of a sample relative to a reference, usually air. DSC functions by applying heat to and maintaining equal temperature between the sample and a reference. As heat applied to both the sample and the reference is increased, deviations of the sample's heat absorption compared with the reference are plotted as curves in a heat flow *vs.* temperature graph (see Figure 2.2). Changes in slope of the plotted line correspond to specific thermal transitions.¹¹⁶ The two prominently utilized thermal transitions in polymer chemistry are melting point and glass transition temperature (T_g), with the latter transition being of greatest interest for this work. T_g is determined via DSC by plotting heat flow (W/g) *vs.* temperature ($^{\circ}$ C) and determining the inflection point of the change in slope of the line, as seen in Figure 2.2.

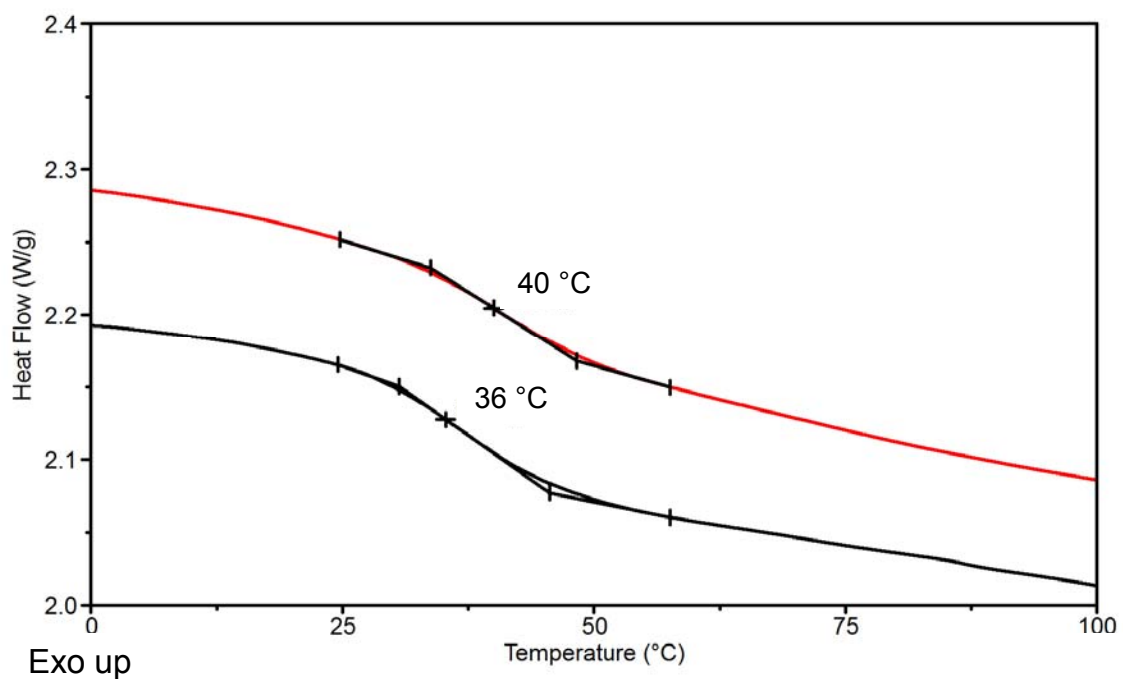


Figure 2.2: DSC overlay of 5 (black line) and 10 (red line) % ^{w/w} fullerene coatings.

A shift in the functional temperature range of the coating can be predicted from a change in the T_g . T_g is the temperature at which an amorphous polymer transitions from a glassy state to a rubbery state upon heating. At temperatures greater than its T_g , a polymer may be elastic, soft, or tacky, such as those used as adhesives. Likewise, at temperatures below its T_g a polymer is more likely to be very fragile and brittle. Since this work modifies MIL-PRF-85285 coatings, it is pertinent to understand that such coatings must withstand temperatures ranging from -50 to 120 °C. Therefore, criteria were established to not significantly alter the T_g , in order to ensure the resulting coating exhibit a functional temperature range within the performance specifications. T_g is a measure of various physical properties which are essential to maintain coating

performance including scratch resistance, adhesion to various substrates, non-cracking, water barrier, and low temperature application. There are methods of modifying a material to shift T_g to a desired range, such as the use of a plasticizer; however, it should be noted that this too is an introduction of yet another extraneous additive and greatly increases the chance that the coating will not satisfy the MIL-PRF-85285 specifications. Table 2.3 presents the T_g of the coatings prepared.

Table 2.3: Glass transition temperatures of formulated coatings.

Additive	T_g (°C)	Additive	T_g (°C)
Control	39	P7	38
Fullerene (1 %)	39	P8	32
Fullerene (5 %)	36	P9	29
Fullerene (10 %)	40	α -Fe	39
P1	23	β -Fe	48
P2	35	γ -Fe	50
P3	37	α -Ni	50
P4	40	β -Ni	50
P5	34	γ -Ni	50
P6	31		

The control coating has a T_g of 39 °C; however, the addition of fullerenes into the polyurethane had little effect on the T_g , with the 5 % and 10 % w/w fullerene loading only slightly affecting the T_g . In general, the incorporation of POMs into the polyurethane at 1 % w/w loading did not have significant impacts on the T_g , however there were exceptions. Samples **P1**, **P6** and **P9** each decreased the T_g when incorporated into the polyurethane, with **P1** resulting in the largest decrease of 16 °C. The addition of **P1** and **P9** into the

coatings resulted in T_g values which are outside of the acceptable range. Incorporation of CDs into the coating resulted in a generally increased T_g . With the exception of α -Fe, the coatings containing CDs exhibited approximately 11 °C increases in T_g , with α -Fe affording no change relative to the control coating. Based on the T_g , it appears that fullerene, **P2-P5** and **P7**, along with α -Fe are well suited additives, while **P6** and **P8**, and remaining CDs may require additional modifications.

2.4 Simulant Degradation on Fullerene Containing Coatings

The surface reactivity of the coatings were investigated by placing CWA simulants on the surface and analyzing the subsequent degradation. Simulants examined for the surface reactivity studies included 2-chloroethyl ethyl sulfide (2-CEES, **12**), 2-chloroethyl phenyl sulfide (2-CEPS, **13**), Demeton-S (Dem, **14**) and Malathion (Mal, **15**), as previously selected in Section 1.9. The use of simulants assures that the analysis of the activity of the coatings is performed as accurately and as safely as possible in the laboratory. Reaction conditions were varied to determine the role of external factors such as time, visible light illumination, atmospheric oxygen concentration and temperature. Illumination with visible light was examined because photocatalytic behavior has been previously documented for several of the additives in this coating set; however, the activity is known only in solution and has not been explored as additives embedded in a polymer. The surface reactivity of all formulated coatings were first investigated in dark conditions. Coatings which contained additives with previously documented photoactive behavior in solutions were further investigated for increased activity due to light

exposure, including specific regions of light irradiation. Similar down-selection was performed for further investigation. Additionally, identification of reaction by-products was performed by GC/MS to quantify simulant degradation and provide further insight into the modes of action through identification of by-products. The detection of specific by-products, such as oxidation by-products, would suggest an oxidative mode of action by the coating.

2.4.1 Effects of light on fullerene coatings

The photocatalytic activity of C₆₀ fullerene loaded coatings at weight percent concentrations of 1, 5, and 10 % were examined. A 175 W commercial mercury vapor light source was employed to illuminate the surfaces and the emission spectrum is presented in Figure 2.3. Except for several bright lines, the light source emits light in the visible region comparable to visible emission of sunlight. Visible spectral band studies were also performed to investigate the effects of certain wavelength regions on the fullerene containing coatings by utilizing polymeric cut-off filters. The percent reduction of simulants on a series of fullerene modified coatings under both dark and light conditions measured by GC/MS is compared in Table 2.4. Percent reduction of CWA simulants on surface was determined by the decrease in GC peak area of the simulants extracted from the coatings containing additives relative to the control.

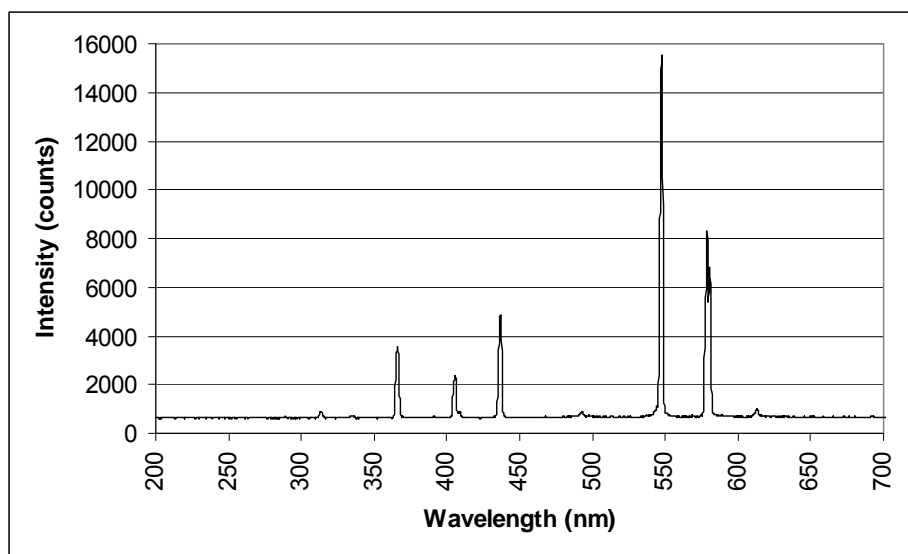


Figure 2.3: Emission spectrum of the mercury vapor light source.

The 2-CEPS degradation was monitored on each of the fullerene containing coatings in dark conditions. The 1 % ^{w/w} fullerene loaded coating was the only surface to exhibit degradation of 2-CEPS under light conditions. Percent reduction of 2-CEPS relative to the control increased with loading upon illumination. Data suggest that the 1 % fullerene loaded coating was particularly photoactive in the decontamination of 2-CEPS; however, no logical conclusion could be drawn as to why the higher loading coatings did not perform equally well under illumination.

Table 2.4: Reduction of simulants in dark and light conditions on fullerene coatings.^a

% Fullerene	2-CEPS		2-CEES		Dem		Mal	
	Dark	Light	Dark	Light	Dark	Light	Dark	Light
1 %	14	41	9	100	73	52	45	11
5 %	17	0	13	14	40	57	19	27
10 %	22	0	17	41	12	59	43	48

^aReduction values reported relative to that of the control coating.

In the absence of light, there were increases in reduction of 2-CEES as the concentration of fullerene in the coating increased. More importantly, irradiation with light resulted in an increase in the degradation of 2-CEES for each loading. Significant increases in 2-CEES reduction were observed in the 1 and 10 % loaded coatings due to irradiation, with quantitative reduction observed at 1 % indicating maximum photocatalytic activity. The lack of photoactivity at the 5 % loading concentration as compared to the 1 % loading is most likely due to aggregation of the fullerene molecules within the coating. Aggregation of fullerene at higher loading concentrations was apparent under an optical microscope at 60x magnification (Figure 2.4). Aggregation of fullerene results in two unfavorable effects. First, aggregation reduces the surface area of additive available at the surface/contaminant boundary. And second, aggregation inhibits singlet oxygen generation by decreasing the lifetime of triplet fullerene through intermolecular quenching.⁸¹

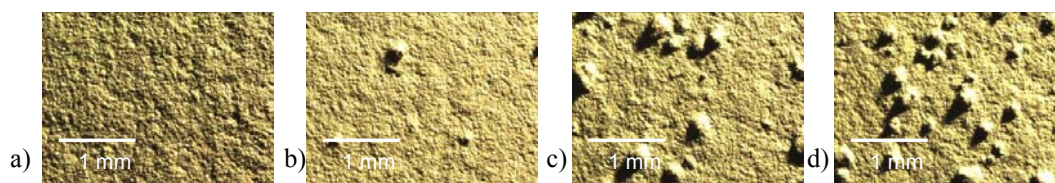


Figure 2.4: Control (a), 1 (b), 5 (c) and 10 (d) % ^{w/w} fullerene coatings at 60x magnification.

All fullerene containing coatings reduced the amount of Dem on the surface relative to the control in both dark and light conditions. Under dark conditions, the reduction of Dem was inversely proportional to loading concentration. Upon

illumination with light, the coatings each exhibited percent reductions around 55 %. Therefore, the relative degradation capability of the 1 % fullerene coating relative to the control actually decreased upon irradiation. Conversely, the 5 and 10 % ^{w/w} fullerene coatings increased their surface activity relative to the control in light conditions. The decrease in the activity of the 1 % fullerene coating may actually be a result of an increase in the photoactivity of the control toward Dem in light conditions as the control contains many pigments, fillers and drying agents. Any increase in activity of the control coating will result in the apparent decrease in activity by the modified coatings because the modified coating's activity is quantified relative to the control. Therefore, the 1 % fullerene coating did not necessarily become less active in the light, but it may have been activated by the light to a lesser degree than the control coating was activated. In summary, the activity obviously resulted from fullerene addition, yet not as photocatalytic as seen earlier.

In the dark, the 1 and 10 % ^{w/w} loaded coatings were more successful in the degradation of Mal than the 5 % ^{w/w} loaded coating. Exposure to light did not significantly improve decontaminating capability of the coatings relative to the control.

Overall, the 1 % coating maintained higher degradation capability of Dem than the control. The increase in activity between dark and light conditions was not as great for the 1 % fullerene coating as that of the control coating. Degradation on the surface of the fullerene coatings were enhanced by irradiation for both of the HD simulants, 2-CEPS and 2-CEES. Both VX simulants were reduced on the fullerene modified coatings in both dark and light conditions. The 1 % ^{w/w} fullerene coating did not exhibit enhanced

degradation of the VX simulants relative to the control after illumination, however the coating maintained reactivity towards Dem and Mal. The surface reactivity of the fullerene containing coatings toward HD simulants were particularly enhanced by exposure to light. Despite no increase from exposure to light relative to the control, the fullerene coatings maintained relatively high reactivity toward VX simulants. Overall, the 1 % ^{w/w} fullerene coating exhibited the optimum reactivity toward both HD and VX simulants.

2.4.2 Effects of specific spectral regions of light on fullerene coatings

The discussion in Section 2.4.1 demonstrated the photocatalytic activity of the fullerene containing coatings toward CWA simulants. In an effort to better understand the mode of action to potentially optimize activity of the self-decontaminating coatings, spectral band studies were conducted. The effects of specific wavelength regions of light on the reaction products of the modified coatings were investigated. The various light conditions included darkness (dark), unfiltered light (no filter), light > 500 nm (yellow filter) and light > 600 nm (red filter). The surface reaction simulant by-products were detected and identified using GC/MS. Figure 2.5 is an absorption spectra overlay of the red and yellow cut-off filters in the visible light region. The yellow filter effectively absorbs wavelengths less than approximately 500 nm and the red filter absorbs light less than approximately 600 nm. Dem was selected for further light specific reaction studies because of its desirable physical properties and identified characteristic reaction products. Additionally, VX agent poses a particular decontamination challenge and the evaluations

of the decontaminating capabilities of the coatings were therefore focused on a VX simulant, specifically Dem. It is believed that Dem mimics the chemical behavior of VX more accurately than Mal.

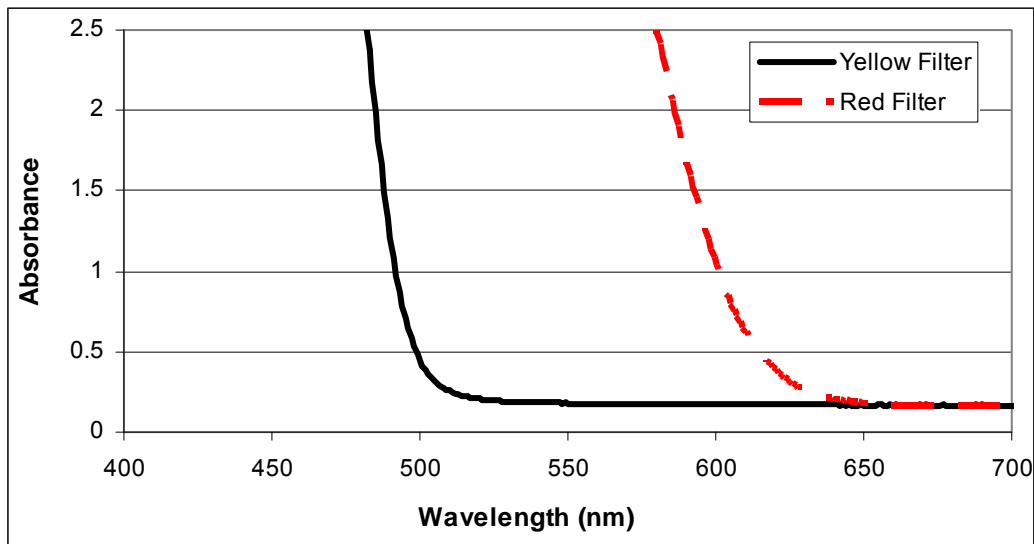


Figure 2.5: Absorption spectra of the red and yellow cut-off filters.

Table 2.5 depicts percent degradation of Dem on fullerene loaded coatings in variable light conditions relative to each control, respectively. The 1 and 5 % ^{w/w} fullerene loaded coatings were examined. The values are given as percent reduction of the quantity of Dem detected by GC/MS relative to the quantity detected on control samples. The Dem was placed on the surface of the coatings and extracted after 5.5 hours. This is in contrast with the previous investigation, where the simulants were on the surface of the coatings for 24 hours prior to extraction.

Table 2.5: Percent reduction of Demeton-S in variable light conditions on fullerene loaded coatings under isothermal conditions.^a

Coating	Dark	Red Filter	Yellow Filter	No Filter
Control	0	0	0	0
1 %	0	10	33	66
5 %	0	7	36	81

^aReduction values reported relative to that of the control coating.

The data presented in Table 2.5 clearly demonstrates the significant effect light of various wavelength regions has on subsequent activity. There was no reduction in the amount of Dem on the surfaces of either 1 or 5 % fullerene under dark conditions. When illuminated with light passing through the red filter, only modest reductions of 10 and 7 % were observed for the 1 and 5 % fullerene loaded coatings, respectively. Percent reductions of approximately 35 % were observed on the fullerene loaded coatings resulting from light that passed through the yellow filter. Both fullerene coatings exhibited their maximum degradation capabilities in the unfiltered light. Each of the degradation percentages are calculated relative to the amount of simulant extracted from control samples under identical illumination conditions. This experimental method correlates the increase in activity observed directly with the increase in light spectrum. The incremental increase in total wavelength exposure correlates with an increase in surface degradation of Dem as well as the visible absorption spectrum of fullerene (Figure 1.11). It was concluded that the entire spectrum of light is contributing to the surface reactivity.

Experiments were conducted in a continuously flowing constant temperature water bath ensuring the temperatures on the surface of each coating under all light

conditions were identical. Water transmits visible light while the surfaces are maintained under isothermal conditions. Calibrated thermocouples were attached to the coating surfaces and the temperature at the surface was monitored over time (Figure 2.6). Surface temperatures were constant at 30 °C at 10 minutes after illumination for samples under each light condition. This demonstrates that difference in coating activity in red filter, yellow filter, or unfiltered light is not the result of heating by the lamp.

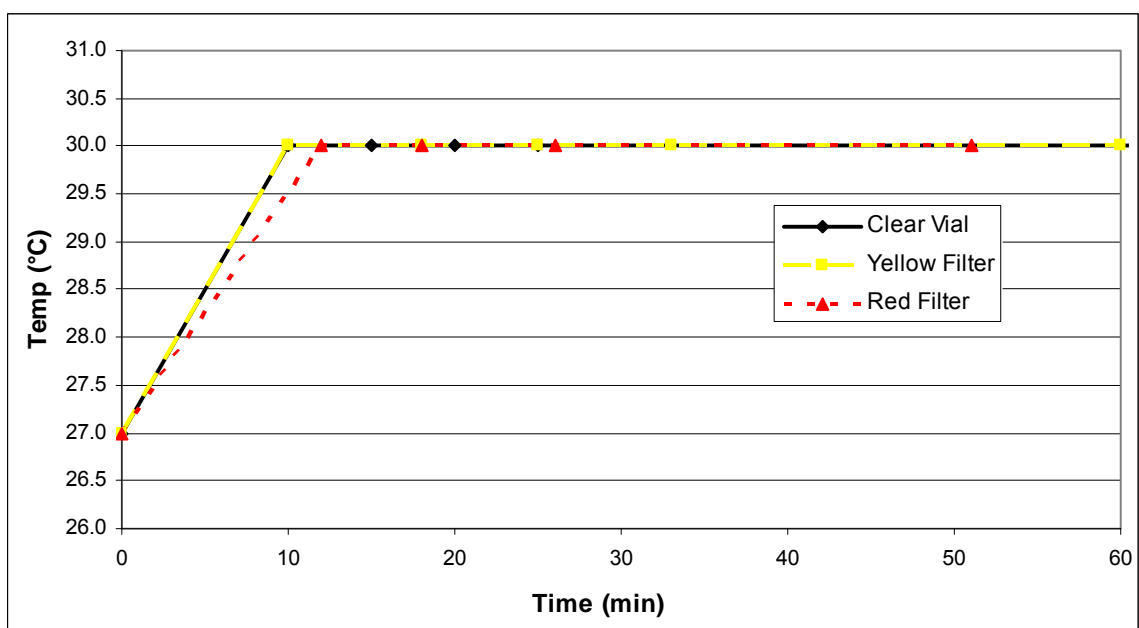


Figure 2.6: Surface temperature of coatings in isothermal photochemical chamber.

2.4.3 By-product analysis of simulant degradation on fullerene coatings

By-products of photocatalytic degradation of Dem on fullerene modified coatings were investigated. Although many products were identified, two products were of particular interest. These products were thiophosphoric acid *S*-(2-ethanesulfonylethyl)

ester *O,O'*-diethyl ester (**16**) and thiophosphoric acid *O,O'*-diethyl ester *S*-vinyl ester (**17**), depicted in Figure 2.7. Both were observed in significant concentrations, were oxidation products, and only observed as a result from exposure to light. Product **16** is the sulfone product of Dem and **17** is an elimination product. *O,O,S*-triethyl ester phosphorothioic acid (**18**), the structure of which is shown in Figure 2.7, was observed in several Dem degradation studies when CD and POM additives were employed.

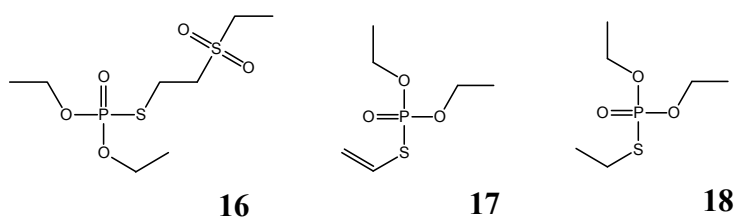


Figure 2.7: Structures of oxidation by-product of Demeton-S.

The formations of **16** and **17** resulting from exposure of fullerene surfaces contaminated with Dem to various spectral regions of light are presented in Table 2.6 as sums of their percent abundance out of the total observed products. **16** and **17** were not observed on coatings in dark or exposed to light with wavelength greater than 600 nm (red filtered). Coatings exposed to light with wavelength greater than 500 nm (yellow filtered) produced minute quantities of **16** and **17**. However, significant quantities of **16** and **17** were observed on coatings exposed to broad spectrum unfiltered light. Light with wavelength less than 500 nm activates fullerene and results in the photocatalytic oxidation of Dem to **16** and **17**. It should be noted that this wavelength specificity only applies to the compounds discussed herein (Section 2.4.3) and do not reflect adversely on

data presented in Table 2.5. The maximum of the absorption spectrum of fullerene in benzene (Figure 1.11) corresponds to the region of light that is most effective in degrading surface residing simulant, which supports that the oxidation products resulted from light activated fullerene in the coating.

Table 2.6: Observed oxidation products of Demeton-S on fullerene loaded coatings under various light conditions given as the percent abundance of total products.

Compound	Illumination Condition	Coating			
		Blank	Control	1 %	5 %
18	Dark	0	0	0	0
	Red Filter	0	0	0	0
	Yellow Filter	0	0	0.2	0.5
	No Filter	0	0	9.1	4.5
19	Dark	0	0	0	0
	Red Filter	0	0	0	0
	Yellow Filter	0	0	0	0.1
	No Filter	0	0	4.4	2.6

2.4.4 Simulant degradation on coatings modified with CD

The surface reactivities of coatings containing CD additives were also investigated. Experimental data displays 2-CEPS, 2-CEES, Dem and Mal reduction for a series of cyclodextrin (CD) modified coatings relative to the control in dark conditions, and is shown in Table 2.7. Reductions of 2-CEPS relative to the control coating were observed in all coatings containing CD additives, with α -Fe, β -Fe, and γ -Fe coatings exhibiting greatest reductions of 64, 23, and 68 %, respectively. The α -Ni, β -Ni, and γ -Ni

demonstrated some reduction of 2-CEPS, albeit less effectively than the Fe series. Overall, the Fe CDs, particularly the α - and γ -Fe cyclodextrins, were most effective in reducing 2-CEPS.

Table 2.7: Simulant reduction on coatings modified with cyclodextrin.^a

CD	2-CEPS	2-CEES	Dem	Mal
α -Fe	64	0	0	34
β -Fe	23	15	0	40
γ -Fe	68	86	0	55
α -Ni	6	34	76	27
β -Ni	24	0	9	43
γ -Ni	28	41	37	61

^aReduction values reported relative to that of the control coating.

The amount of 2-CEES was reduced on four of the six CD coatings investigated (Table 2.7). The γ -Fe containing coating reduced the amount of 2-CEES on the surface 86 %, while the γ -Ni coating exhibited a reduction of only 41 %. γ -Fe and γ -Ni each exhibited the greatest overall activity against 2-CEES. Interestingly, α -Fe showed no reduction of 2-CEES, while the same coating very effectively reduced 2-CEPS. No direct correlation was observed between the diameter of the ring and the reduction of either 2-CEPS or 2-CEES, although the γ CDs most effectively degraded both simulants. This illustrates the importance of using multiple simulants to best accurately represent the reactivity of the actual agent.

The amount of surface residing Dem was reduced in three of the coatings, with α -Ni, β -Ni, and γ -Ni each exhibiting significant reduction of Dem on the surface. There were no significant reductions of Dem observed on the coatings containing the Fe-CD

additives. It is notable that each of the Ni-containing CDs exhibited decontamination of Dem while each of the Fe-containing counterparts did not. It was concluded that Ni is better suited to coordinate with Dem, facilitating subsequent chemical degradation.

Each of the CD additives exhibited improved decontamination of Mal, when compared to control. The α -, β -, and γ -Fe containing CDs achieved significant reductions of 34, 40, and 55 %, respectively. The α -, β -, and γ -Ni CD loaded coatings also exhibited respective reductions of 27, 43, and 61 %. The reduction of Mal followed a pattern of efficacy in the order of $\gamma > \beta > \alpha$, regardless of the metal in the complex, with γ -Fe and γ -Ni showing greatest promise of success. Clearly, degradation of Mal is dependent on the diameter of the ring and suggests that Mal must physically approach and fit-into the CD cavity to some degree for the reaction to occur, otherwise smaller diameter rings would exhibit similar activity.

For cyclodextrins, 2-CEPS and 2-CEES were significantly reduced by the additives γ -Fe and γ -Ni. γ -Fe modified coatings most effectively reduced the HD simulants at 68 and 86 %, respectively, yet, γ -Fe was totally ineffective in the reduction of Dem. γ -Ni exhibited more modest 2-CEPS and 2-CEES reductions of 28 and 41 %, respectively. However, γ -Ni reduced both Dem and Mal by 37 and 61 %, respectively. γ -Ni is the only cyclodextrin additive to significantly reduce all four of the simulants examined. As a result, γ -Ni appeared to be the most active additive among the six cyclodextrins and was selected for further examination and analysis.

2.4.5 Simulant degradation on coatings modified with POMs

The series of POMs incorporated into coatings are shown in Table 2.1. The POMs examined in this study were synthesized following previously published procedures.¹¹⁷⁻¹¹⁹ Table 2.8 presents the percent reductions of CWA simulants of the POM containing coatings as compared to a control coating in dark conditions.

Table 2.8: Simulant reduction on POM modified coatings.^a

Additive	2-CEPS	2-CEES	Dem	Mal
Control	0	0	0	0
P1	0	0	77	21
P2	7	0	75	18
P3	34	0	30	53
P4	0	0	0	0
P5	8	5	0	0
P6	0	0	50	0
P7	0	0	61	0
P8	0	35	0	0
P9	39	0	0	0

^aReduction values reported relative to that of the control coating.

Reductions in 2-CEPS were observed in four POM modified coatings when compared to the control. The four effective additives were **P2**, **P3**, **P5** and **P9**, of which **P3** and **P9** exhibited the most significant observed reduction in 2-CEPS. The **P8** modified coating demonstrated the only significant 2-CEES reduction at 35 %. Significant reductions of Dem were observed with **P1**, **P2**, **P6** and **P7**. These exhibited reductions relative to the control of 77, 75, 50, and 61 %, respectively. Likewise, reduction of Mal was observed on three of the nine coatings investigated. However, only **P3** displayed a significant reduction of 53 %.

Coatings containing additives **P1**, **P2** and **P3** were the only surfaces to exhibit improved decontamination of both Dem and Mal compared to the control coating. **P1**, **P2**, and **P3** all exhibit the Dawson crystal structure. Of these, **P1** best reduced Dem and **P3** best reduced Mal. **P3** also exhibited significant reduction of the simulant 2-CEPS. In consideration of both classes of simulants, **P3** exhibited the most universal decontamination ability of all the POM additives examined. **P3** exhibited 34, 30, and 53 % reductions of 2-CEPS, Dem, and Mal, respectively; however, **P3** failed to decontaminate 2-CEES. Regardless, this result may be insignificant as previous work has shown that activity across a collection of simulants better represents CWA degradation than performance against any individual simulant.⁵⁴ Interestingly, POMs metalated with Ni were the most active and this also corresponds to the activity that the CD containing coatings exhibited, where those metalated with Ni were most active. In summary, of all POM additives examined, **P3** (α_2 -K₈P₂W₁₇O₆₁(Ni²⁺·OH₂)·17H₂O) has emerged as the most promising candidate for further investigation towards an effective additive to impart universal decontamination to a coating.

2.4.6 Effects of light on CD & POM modified coatings

The CD additive γ -Ni and the POM additive **P3** have each emerged as the most promising of these two classes and were therefore subjected to additional photoactivity investigations. Coatings containing 1 % ^{w/w} γ -Ni and **P3**, respectively, were subjected to CWA simulants and then placed under a UV-visible light source for analysis of simulant degradation. 2-CEPS and Dem were selected as representative simulants, since the pair

exhibited the optimum combination of physical characteristics and degradation challenge of the simulants. Table 2.9 displays a comparison of the degradation results obtained for the simulants under both light and dark conditions. Samples were extracted with acetonitrile for GC/MS analysis 24 hours after the simulants were applied to the surfaces.

Table 2.9: Percent reduction of 2-CEPS and Demeton-S by CD and POM modified coatings in dark and light conditions at 24 hours.^a

	2-CEPS		Demeton-S	
	Dark	Light	Dark	Light
γ -Ni	28	51	37	69
P3	34	74	30	58

^aReduction values reported relative to that of the control coating.

The degradation of 2-CEPS on the coating surfaces increased for both the γ -Ni and **P3** modified coatings, relative to the control coatings, following UV-vis irradiation. γ -Ni had previously exhibited a 28 % surface reduction of 2-CEPS under dark conditions. An increase in reduction to 51 % was observed upon exposure to broad spectrum light. The percent reduction of 2-CEPS on a **P3** loaded coating in dark conditions was 34 %; however, the value increased to 74 % upon exposure to light. In both cases, the addition of light demonstrated significant enhancement in surface activity.

Both γ -Ni and **P3** exhibited significant increases in degradation of Dem resulting from exposure to light. Percent reductions of Dem on the surface of γ -Ni and **P3** in dark conditions were 37 and 30, respectively. The same coatings exposed to light resulted in significant enhancements in reductions to 69 and 58 %, respectively, which confirmed that indeed light dependent activity was occurring.

Furthermore, specific regions of light were investigated for a more precise understanding of the photoactivity occurring and results are shown in Table 2.10. The red filter and yellow filter columns refer to the filters whose absorption spectrum was previously presented in Figure 2.5. Dem was applied to the surface of each coating and extracted after 5.5 hours. The shortened incubation time explains why the γ -Ni and **P3** samples exhibited no degradation in the dark, while in Table 2.9 both exhibited activity in the dark after 24 hours.

Table 2.10: Reduction of Demeton-S on CD and POM coatings in various light conditions at 5.5 hours.^a

	Dark	Red Filter	Yellow Filter	No Filter
γ -Ni	0	0	0	38
P3	0	0	0	25

^aReduction values reported relative to that of the control coating.

The degradation of Dem on the CD and POM modified coatings resulted in the formation of *O,O,S*-triethyl ester phosphorothioic acid (**18**). The formation of **18** on γ -Ni and **P3** is believed to result from a mechanism different from that of the fullerene containing coatings. The amount of **18** formed from the reactions on both the CD and POM modified coatings remains relatively constant whether the surfaces are exposed to dark, light, yellow filter, or red filter conditions. The degree to which **18** was formed on CD and POM modified coatings examined under identical isothermal conditions was found to be independent of exposure to light.

2.4.7 Effects of atmospheric oxygen

The degradation of surface contaminants on fullerene, γ -Ni and **P3** coatings in oxygen depleted atmospheres were also investigated. Samples were placed in 1.5 mL Eppendorf tubes which were sealed under either ambient air or were purged for 2 minutes with a flow of nitrogen gas. The nitrogen purged atmospheres resulted in a sample environment of greatly reduced oxygen content. Figure 2.8 displays, as a percentage, the increase in the surface reduction of Dem on each coating formulation in ambient air relative to the reduction of the identical coating in a nitrogen purged atmosphere. The graph shows percent improvement in degradation observed for coatings in ambient air relative to coatings maintained in a purged nitrogen atmosphere. All samples were illuminated by unfiltered light from the mercury vapor lamp and maintained at constant temperature via the aforementioned water bath during the 5.5 hour exposure.

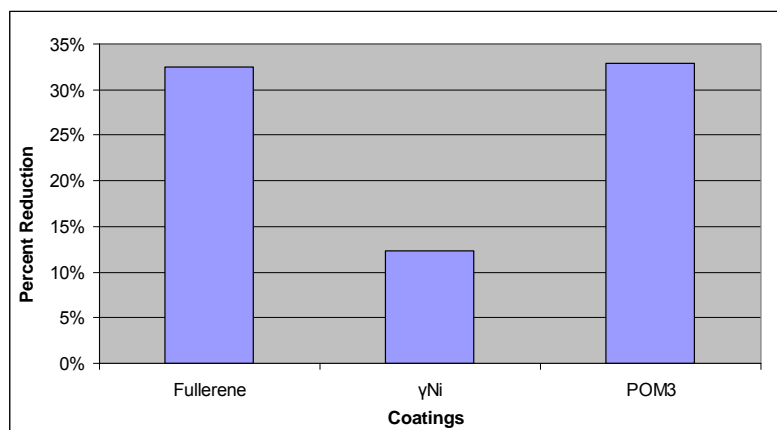


Figure 2.8: Percent reduction of Demeton-S on coatings in ambient air relative to coatings in a nitrogen purged atmosphere.

All coatings containing additives exhibited an increase in reduction of Dem on the surface in ambient atmospheres, compared to corresponding reductions in oxygen depleted atmospheres. This suggested that regardless of additive, atmospheric oxygen facilitated reaction with surface residing Dem. The coating containing γ -Ni exhibited a slight increase in reactivity under an ambient atmosphere as compared to the γ -Ni coating in oxygen-depleted conditions. Conversely, the fullerene and **P3** coatings exhibited dramatic surface degradation capabilities in the oxygen rich environments compared with their oxygen depleted counterparts. This suggests that fullerene and **P3** are more dependent upon atmospheric oxygen in the catalytic breakdown of surface Dem. Overall, a higher concentration of oxygen in the air immediately surrounding the coating-contaminant interface increases the degree to which the simulant will degrade over time, regardless of the additive in the coating. However, fullerene and **P3** additives demonstrated significant increases in activity from an increase in atmospheric oxygen and perhaps function through a mechanism which utilizes ambient oxygen to more rapidly degrade surface contaminants.

3. Conclusion

A series of novel surface active catalytic additives were selected, synthesized, screened and incorporated into a commercial resin system and the resulting coatings demonstrated significant surface reactivity towards CWA simulants. Incorporation of additives at low concentration allowed for retention of the physical properties of the coating system while adding functionality. Of the formulated coatings, the fullerenes and cyclodextrin containing coatings exhibited the most effective universal decontamination toward all four CWA simulants employed in this study. Of the fullerene containing coatings, the 1 % ^{w/w} loading exhibited higher reactivity relative to other loading concentrations while the γ -CDs performed the best of the cyclodextrin containing coatings. The fullerene containing coatings exhibited notable photocatalytic behavior. An incremental increase in broad spectrum UV-vis exposure correlated with an increase in surface degradation of Dem. It appears the entire spectrum of UV-vis light is contributing to the photocatalytic activation of fullerene. Exposure of fullerene containing coatings contaminated with Demeton-S to light with wavelength less than 500 nm resulted in readily identifiable oxidation by-products in significant quantities. In a reduced O₂ atmosphere, photocatalytic activity was greatly reduced. This study demonstrated evidence of photocatalytic oxidation of surface contaminants by coatings containing C₆₀ fullerene through a singlet oxygen mediated mechanism.

4. Experimental Methods

4.1 Experimental Overview

Unless otherwise noted, additives were incorporated into a commercial coating at 1 % ^w/_w. These coatings were characterized and subjected to a series of decontamination challenges and subsequent GC/MS analysis to determine the activity of the surface of the resultant coating.

4.2 Coating Preparation

Chemical additives were thoroughly mixed into commercially available paint formulations (MIL-PRF-85285) manufactured by DEFT Inc. (Irvine, CA). MIL-PRF-85285 is a two component commercial polyurethane. The components were vigorously mixed prior to incorporation of additives to ensure even dispersion of pigments and fillers. The two components were then mixed together in a 3:1 ratio, and additives were then incorporated at appropriate % ^w/_w concentrations. MIL-PRF-85285 coating is composed of 50 % ^w/_w solid (resin, pigments and fillers) and 50 % ^w/_w solvent. The weight of the solid portion was used to calculate the necessary amount of additive to achieve desired concentrations. Mixing methods included both mechanical stirring and vortex mixing to achieve uniform dispersion of additives. Formulated coatings were applied to pre-cleaned aluminum foil sheets and aluminum Q-panels for surface

decontamination studies. The air-spray application employing a Dayton™ 4RR09 Air brush at 25 psi was performed to apply uniform coatings. Coatings were allowed to cure under ambient conditions for at least 24 hours prior to any surface characterization. Coating thicknesses for all samples were approximately 4 mils (100 µm).

4.3 Chemical Decontamination Challenge

Coatings were evaluated for chemical decontamination ability, using four chemical simulants selected based on their chemical and physical similarities to the agents HD and VX. For each coating formulation, four circular coupons (2 cm²) were cut, onto which a 0.5 µL aliquot of each simulant was applied and placed into a 1.5 mL Eppendorf tube and then sealed. Two controls were prepared for each simulant tested. These included an empty Eppendorf tube (with no coating sample) loaded with 0.5 µL of simulant and a control coating (no additive) loaded with identical amount of simulant. The simulant was allowed to reside on the surface of the coatings for either 5.5 hours or 24 hours as indicated. Additionally, several independent variables were controlled such as light exposure, temperature, and atmospheric composition. A 1 mL aliquot of acetonitrile was added to the sample and vortexed for 20 seconds to extract the simulant and degradation products. The solution was then collected with a 1 mL syringe, and expelled through a 0.2 µm syringe filter into a 1.5 mL GC/MS autoinjector vial equipped with a Teflon septa top for subsequent analysis.

4.4 GC/MS Analysis

Gas chromatography/mass spectroscopy (GC/MS) was employed to identify and quantify simulant degradation products. The GC/MS system consisted of an Agilent 7890A gas chromatograph equipped with an Agilent 5975C mass selective detector operating in electron ionization mode and an Agilent 7693A autoinjector. The column utilized was an Agilent HP-5MS (5 % phenyl) methylpolysiloxane film. The carrier gas was helium with a flow rate of 1 mL·min⁻¹. The injection volume was 1 µL with a split injection ratio of 20:1. The temperature program had an initial temperature of 100 °C for one minute, then a 25 °C·min⁻¹ ramp to 130 °C followed by a 15 °C·min⁻¹ ramp to 250 °C with a one minute post run hold at 300 °C. Injection temperature, MS quad temperature, and source temperatures were 300, 150 and 230 °C, respectively. The solvent delay was set at 1.5 minutes and the detector was set to scan a mass range of 20 to 350 *m/z*. A sample mass spectrum of Demeton-S, with the major ion peaks labeled, is shown in Figure 4.1.

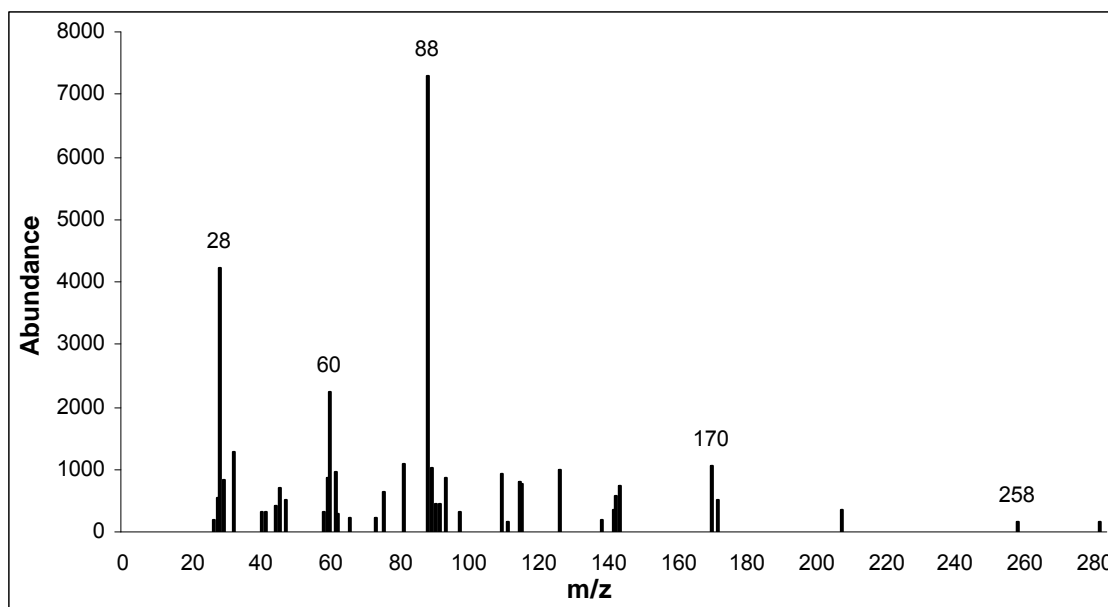


Figure 4.1: Mass spectrum of Demeton-S.

4.5 UV-Vis Irradiation

A commercially available residential-type 175 Watt mercury vapor light source was employed for illumination studies. The emission spectrum of the light source is presented in Figure 2.3. An isothermal photochemical chamber was specifically developed to maintain constant temperature for the duration of the experiments. The isothermal photochemical chamber consisted of a continuously flowing water bath and was capable of maintaining temperatures from 15 to 30 °C. Polymeric filters in the UV-visible range purchased from Roscolux were employed to examine the effect of specific wavelengths of energy. The filters utilized exhibit absorption spectra which were displayed in Figure 2.5.

4.6 Differential Scanning Calorimetry

All coatings were peeled from their respective aluminum backings prior to DSC analysis. A TA Instruments Q20 differential scanning calorimeter equipped with a RCS90 cooling system was employed. Under a nitrogen flow of 50 mL·min⁻¹, the DSC was first cooled to -75 °C at a rate of 5 °C·min⁻¹. The temperature was then ramped from -75 °C to 150 °C at a rate of 20 °C·min⁻¹. Two such cooling and heating temperature ramps were successively performed. T_g was measured from the second heating scan to eliminate any contamination of entrapped volatile and low molecular weight by-products, as well as to demonstrate reversibility. Glass transition temperature (T_g) measurements were determined at the inflection point of the heat capacity shift of the coating using Universal Analysis 2000 software.

4.7 Contact Angle Analysis

Surface energy and contact angle measurements were performed using a VCA 2500 video contact angle system (AST Products, Inc., Billerica, MA) and the sessile drop technique was employed. The sessile drop technique involves the measurement of the contact angle of a static drop of liquid on a flat surface. The drop was deposited onto the surface through contact of a pendant drop with the surface. Adhesion to the surface pulls the drop from the syringe tip. Multiple probe solvents exhibiting a range of surface tensions were applied. The multiple probe liquids utilized were triple distilled water, ethylene glycol, diiodomethane, and *n*-hexadecane. A high resolution image of the interface was captured three seconds after solvent application, and contact angles were

subsequently measured on VCA OptimaXE software. For each liquid, three replicate measurements were performed. From the contact angle, coating surface energy was independently calculated via the Zisman and Owens methods.

4.8 Nitrogen Purging

For each coating under examination, two samples were placed in 1.5 mL Eppendorf tubes and simulants were applied to the surface. One Eppendorf tube was purged with house nitrogen supplied by liquid boil-off for 2 minutes prior to being sealed. The analogous Eppendorf tube was sealed containing ambient air. The samples were incubated for 5.5 hours and analyzed following the procedure previously described in Section 4.3.

References

References

1. Suzuki, T.; Morita, H.; Ono, K.; Maekawa, K.; Nagai, R.; Yazaki, Y.; Nozaki, H.; Aikawa, N.; Shinozawa, Y.; Hori, S.; Fujishima, S.; Takuma, K.; Sagoh, M. Sarin poisoning in Tokyo subway. *Lancet* **1995**, *345*, 980-981.
2. Morita, H.; Yanagisawa, N.; Nakajima, T.; Shimizu, M.; Hirabayashi, H.; Okudera, H.; Nohara, M.; Midorikawa, Y.; Mimura, S. Sarin poisoning in Matsumoto, Japan. *Lancet* **1995**, *346*, 290-293.
3. Talmage, S. S.; Watson, A. P.; Hauschild, V.; Munro, N. B.; King, J. Chemical warfare agent degradation and decontamination. *Curr. Org. Chem.* **2007**, *11*, 285-298.
4. Munro, N. B.; Ambrose, K. R.; Watson, A. P. Toxicity of the organophosphate chemical warfare agents GA, GB, and VX - Implications for public protection. *Environ. Health Perspect.* **1994**, *102*, 18-38.
5. USACMLS. *Multiservice tactics, techniques, and procedures for chemical, biological, radiological, and nuclear decontamination*. 2006.
6. USAMRICD. *Medical Management of Chemical Casualties Handbook* Fourth Edition ed.; 2007.
7. *NATO Handbook on the Medical Aspects of NBC Defensive Operations AMedP-6(B)*. Department of the Army, the Navy, and the Air Force: Washington, DC, 1996.
8. Olajos, E. J.; Salem, H. Riot control agents: Pharmacology, toxicology, biochemistry and chemistry. *J. Appl. Toxicol.* **2001**, *21*, 355-391.
9. Romano, J. A.; Lukey, B. J.; Salem, H. *Chemical Warfare Agents: Chemistry, Pharmacology, Toxicology, and Therapeutics*. 2nd ed.; CRC Press: 2008; p 723.
10. Cooper, C. E.; Brown, G. C. The inhibition of mitochondrial cytochrome oxidase by the gases carbon monoxide, nitric oxide, hydrogen cyanide and hydrogen sulfide: chemical mechanism and physiological significance. *J. Bioenerg. Biomembr.* **2008**, *40*, 533-539.

11. *Toxicological Profile for Cyanide*; ATSDR, U.S. Department of Health and Human Services: Atlanta, GA, 2006.
12. Keren, D.; McCarthy, J.; Mazal, H. The ruins of the gas chambers: A forensic investigation of crematoriums at Auschwitz i and Auschwitz-Birkenau. *Holocaust and Genocide Studies* **2004**, *18*, 68-103.
13. Borak, J.; Diller, W. F. Phosgene exposure: Mechanism of injury and treatment strategies. *Journal of Occupational and Environmental Medicine* **2001**, *43*, 110-119.
14. Das, R.; Blanc, P. D. Chlorine gas exposure and the lung: A review. *Toxicology and Industrial Health* **1993**, *9*, 439-455.
15. Winder, C. The toxicology of chlorine. *Environ. Res.* **2001**, *85*, 105-114.
16. Diller, W. F. Pathogenesis of phosgene poisoning. *Toxicology and Industrial Health* **1985**, *1*, 7-15.
17. Meakins, J. C.; Priestley, J. G. The after-effects of chlorine gas poisoning. *Canadian Medical Association Journal* **1919**, *9*, 968-974.
18. Szinicz, L. History of chemical and biological warfare agents. *Toxicology* **2005**, *214*, 167-181.
19. Watson, A. P.; Griffin, G. D. Toxicity of vesicant agents scheduled for destruction by the chemical stockpile disposal program. *Environ. Health Perspect.* **1992**, *98*, 259-280.
20. Wormser, U. Toxicology of mustard gas. *Trends Pharmacol. Sci.* **1991**, *12*, 164-167.
21. Bismuth, C.; Borron, S. W.; Baud, F. J.; Barriot, P. Chemical weapons: documented use and compounds on the horizon. *Toxicol. Lett.* **2004**, *149*, 11-18.
22. OPCW *On the Implementation of the Convention on the Prohibition of the Development, Production, Stockpiling and Use of Chemical Weapons and on their Destruction in 2008*; Organisation for the Prohibition of Chemical Weapons: 2009; p 65.
23. Korkmaz, A.; Yaren, H.; Topal, T.; Oter, S. Molecular targets against mustard toxicity: Implication of cell surface receptors, peroxynitrite production, and PARP activation. *Arch. Toxicol.* **2006**, *80*, 662-670.
24. Hosseini-khalili, A.; Haines, D. D.; Modirian, E.; Soroush, M.; Khateri, S.; Joshi, R.; Zendehtdel, K.; Ghanei, M.; Giardina, C. Mustard gas exposure and

- carcinogenesis of lung. *Mutation Research/Genetic Toxicology and Environmental Mutagenesis* **2009**, 678, 1-6.
25. Yamakido, M.; Ishioka, S.; Hiyama, K.; Maeda, A. Former poison gas workers and cancer: Incidence and inhibition of tumor formation by treatment with biological response modifier N-CWS. *Environ. Health Perspect.* **1996**, 104, 485-488.
 26. Adachi, S.; Takemoto, K. Occupational lung cancer. A comparison between humans and experimental animals. *Japanese Journal of Industrial Health* **1987**, 29, 345-357.
 27. Davis, K. G.; Aspera, G. Exposure to liquid sulfur mustard. *Annals of Emergency Medicine* **2001**, 37, 653-656.
 28. Russell, D.; Blaine, P. G.; Rice, P. Clinical management of casualties exposed to lung damaging agents: A critical review. *Emergency Medicine Journal* **2006**, 23, 421-424.
 29. Mileson, B. E.; Chambers, J. E.; Chen, W. L.; Dettbarn, W.; Ehrich, M.; Eldefrawi, A. T.; Gaylor, D. W.; Hamernik, K.; Hodgson, E.; Karczmar, A. G.; Padilla, S.; Pope, C. N.; Richardson, R. J.; Saunders, D. R.; Sheets, L. P.; Sultatos, L. G.; Wallace, K. B. Common mechanism of toxicity: A case study of organophosphorus pesticides. *Toxicol. Sci.* **1998**, 41, 8-20.
 30. Jokanovic, M. Current understanding of the mechanisms involved in metabolic detoxification of warfare nerve agents. *Toxicol. Lett.* **2009**, 188, 1-10.
 31. Cholinesterase Inhibitors Including Insecticides and Chemical Warfare Nerve Agents Part 2: What are cholinesterase inhibitors? *Periodical* [Online], 2007. http://www.atsdr.cdc.gov/csem/cholinesterase/cholinesterase_inhibitors.html (accessed February 23, 2011).
 32. Pope, C.; Karanth, S.; Liu, J. Pharmacology and toxicology of cholinesterase inhibitors: uses and misuses of a common mechanism of action. *Environ. Toxicol. Pharmacol.* **2005**, 19, 433-446.
 33. Tucker, J. B. *War of Nerves: chemical warfare from World War I to Al-Qaeda*. 1st ed.; Pantheon Books: New York, 2006; pp 479.
 34. Lefebure, V. *The Riddle of the Rhine*. The Chemical Foundation, Inc.: New York City, 1923; pp 282.
 35. Despretz, C. *Ann. Chim. Phys* **1822**, 1, 437.

36. Guthrie, F. Q. *J. Chem. Soc* **1859**, 12, 109.
37. Meyer, V. Ueber Thiodiglykolverbindungen. *Ber. Deut. Chem. Ges* **1886**, 19, 3259-3266.
38. Benschop, H. P.; Van Der Schans, G. P.; Noort, D.; Fidder, A.; Mars-Groenendijk, R. H.; De Jong, L. P. A. Verification of exposure to sulfur mustard in two casualties of the Iran-Iraq conflict. *J. Anal. Toxicol.* **1997**, 21, 249-251.
39. Ember, L. Chemical weapons - Residues verify Iraqi use on Kurds. *Chem. Eng. News* **1993**, 71, 8-9.
40. Okumura, T.; Takasu, N.; Ishimatsu, S.; Miyanoki, S.; Mitsunashi, A.; Kumada, K.; Tanaka, K.; Hinohara, S. Report on 640 victims of the Tokyo subway sarin attack. *Annals of Emergency Medicine* **1996**, 28, 129-135.
41. Zurer, P. Japanese cult used VX to slay member. *Chem. Eng. News* **1998**, 76, 7.
42. Yang, Y. C.; Baker, J. A.; Ward, J. R. Decontamination of chemical warfare agents. *Chem. Rev. (Washington, DC, U. S.)* **1992**, 92, 1729-1743.
43. Fitch, J. P.; Raber, E.; Imbro, D. R. Technology Challenges in Responding to Biological or Chemical Attacks in the Civilian Sector. *Science* **2003**, 302, 1350-1354.
44. Fielding, G. *Field Decontamination Studies With Chemical Warfare Decontaminating Solution DS2*; Naval Research Laboratory: Washington, DC, 1964; p 29.
45. Modec, I. <http://deconsolutions.com/mdf200.html> (accessed Mar. 3, 2011).
46. Reynolds, C. M.; Ringelberg, D. B.; Perry, L. B.; Wagner, G. W. Performance of an emerging all-weather decontamination solution against nerve and mustard agent simulants at subfreezing temperatures. *Cold Regions Science and Technology* **2008**, 52, 244-253.
47. Wagner, G. W.; Procell, L. R.; Yang, Y. C.; Bunton, C. A. Molybdate/peroxide oxidation of mustard in microemulsions. *Langmuir* **2001**, 17, 4809-4811.
48. Wagner, G. W.; Yang, Y. C. Rapid nucleophilic/oxidative decontamination of chemical warfare agents. *Ind. Eng. Chem. Res.* **2002**, 41, 1925-1928.
49. Wagner, G. W.; Procell, L. R.; Sorrick, D. C.; Lawson, G. E.; Wells, C. M.; Reynolds, C. M.; Ringelberg, D. B.; Foley, K. L.; Lumetta, G. J.; Blanchard, D. L. All-Weather Hydrogen Peroxide-Based Decontamination of CBRN Contaminants. *Ind. Eng. Chem. Res.* **2010**, 49, 3099-3105.

50. Wagner, G. W. P., L.R.; Sorrick, D.C.; Hess, Z.A.; Gehring, D.G.; Henderson, V.D.; Brickhouse, M.D.; Rastogi, V.K.; Turetsky, A.L.; Pfarr, J.W.; Dean-Wilson, A.M.; Kuhstoss, S.M.; Schilling, A.S. *Development of New Decon Green: A How-To Guide for the Rapid Decontamination of CARC Paint*; U.S. Army Research, Development and Engineering Command: Edgewood Chemical Biological Center, 2008; p 51.
51. Wagner, G. W. P., L.R.; Sorrick, D.C.; Hess, Z.A.; Gehring, D.G.; Henderson, V.D.; Brickhouse, M.D. *Decon Green*; Edgewood Chemical Biological Center: Aberdeen Proving Ground MD, 2004; p 4.
52. Reynolds, C. M. R., D.B; Perry, L.B *Efficacy of DECON Green against VX Nerve and HD Mustard Simulants at Subfreezing Temperatures*; Engineering Research and Development Center: Hanover NH Cold Regions Research and Engineering Lab, 2006; p 25.
53. Wagner, G. W. B., P.W.; Procell, L.R.; Sorrick, D.C.; Henderson, V.D.; Turetsky, A.L.; Rastogi, V.K.; Yang, Y.C. *DECON GREEN Development and Chemical Biological Agent Efficacy Testing*; Edgewood Chemical Biological Center: Aberdeen Proving Ground MD, 2004; p 20.
54. Bartelt-Hunt, S. L.; Knappe, D. R. U.; Barlaz, M. A. A review of chemical warfare agent simulants for the study of environmental behavior. *Critical Reviews in Environmental Science and Technology* **2008**, *38*, 112-136.
55. Anslow, W. P.; Karnofsky, D. A.; Jager, B. V.; Smith, H. W. The intravenous, subcutaneous and cutaneous toxicity of bis(beta-chloroethyl) sulfide (mustard gas) and of various derivatives. *J. Pharmacol. Exp. Ther.* **1948**, *93*, 1-9.
56. Yang, Y. C.; Szafraniec, L. L.; Beaudry, W. T.; Ward, J. R. Kinetics and mechanism of the hydrolysis of 2-chloroethyl sulfides. *J. Org. Chem.* **1988**, *53*, 3293-3297.
57. Wagner, G. W.; Bartram, P. W. Reactions of the mustard simulant 2-chloroethyl phenyl sulfide with self-decontaminating sorbents. A ¹³C MAS NMR study. *J. Mol. Catal. A: Chem.* **1996**, *111*, 175-180.
58. Wagner, G. W.; Bartram, P. W. Reactions of VX, HD, and their simulants with NaY and AgY zeolites. Desulfurization of VX on AgY. *Langmuir* **1999**, *15*, 8113-8118.
59. Jaeger, D. A.; Roberts, T. L.; Zelenin, A. K. Quaternary ammonium O,O'-dialkylphosphorodithioate surfactants and their reactions with 2-chloroethyl phenyl sulfide, a mustard simulant. *Colloids and Surfaces A: Physicochemical and Engineering Aspects* **2002**, *196*, 209-216.

60. Yang, Y. C.; Szafraniec, L. L.; Beaudry, W. T.; Davis, F. A. A comparison of the oxidative reactivities of mustard (2,2'-dichlorodiethyl sulfide) and bivalent sulfides. *J. Org. Chem.* **1990**, *55*, 3664-3666.
61. Wagner, G. W.; Koper, O. B.; Lucas, E.; Decker, S.; Klabunde, K. J. Reactions of VX, GD, and HD with Nanosize CaO: Autocatalytic Dehydrohalogenation of HD. *J. Phys. Chem. B* **2000**, *104*, 5118-5123.
62. Boring, E.; Geletii, Y. V.; Hill, C. L. A Homogeneous Catalyst for Selective O₂ Oxidation at Ambient Temperature. Diversity-Based Discovery and Mechanistic Investigation of Thioether Oxidation by the Au^{III}Cl₂NO₃(thioether)/O₂ System. *J. Am. Chem. Soc.* **2001**, *123*, 1625-1635.
63. Martyanov, I. N.; Klabunde, K. J. Photocatalytic Oxidation of Gaseous 2-Chloroethyl Ethyl Sulfide over TiO₂. *Environ. Sci. Technol.* **2003**, *37*, 3448-3453.
64. Wu, K. H.; Yu, P. Y.; Yang, C. C.; Wang, G. P.; Chao, C. M. Preparation and characterization of polyoxometalate-modified poly(vinyl alcohol)/polyethyleneimine hybrids as a chemical and biological self-detoxifying material. *Polym. Degrad. Stab.* **2009**, *94*, 1411-1418.
65. Kleinhammes, A.; Wagner, G. W.; Kulkarni, H.; Jia, Y.; Zhang, Q.; Qin, L.-C.; Wu, Y. Decontamination of 2-chloroethyl ethylsulfide using titanate nanoscrolls. *Chem. Phys. Lett.* **2005**, *411*, 81-85.
66. McDaniel, C. S.; McDaniel, J.; Wales, M. E.; Wild, J. R. Enzyme-based additives for paints and coatings. *Prog. Org. Coat.* **2006**, *55*, 182-188.
67. Ziegler, W.; Engelhardt, G.; Wallnoefer, P. R.; Oehlmann, L.; Wagner, K. Degradation of demeton S-methyl sulfoxide (Metasystox R) by soil microorganisms. *J. Agric. Food Chem.* **1980**, *28*, 1102-1106.
68. *Boll Weevil Eradication Program Fact Sheet*; USDA, Animal and Plant Health Inspection Service: 2007.
69. Wynne, J. H.; Pant, R. R.; Jones-Meehan, J. M.; Phillips, J. P. Preparation and evaluation of nonionic amphiphilic phenolic biocides in urethane hydrogels. *J. Appl. Polym. Sci.* **2008**, *107*, 2089-2094.
70. Pant, R. R.; Buckley, J. L.; Fulmer, P. A.; Wynne, J. H.; McCluskey, D. M.; Phillips, J. P. Hybrid siloxane epoxy coatings containing quaternary ammonium moieties. *J. Appl. Polym. Sci.* **2008**, *110*, 3080-3086.

71. Kurt, P.; Wood, L.; Ohman, D. E.; Wynne, K. J. Highly effective contact antimicrobial surfaces via polymer surface modifiers. *Langmuir* **2007**, *23*, 4719-4723.
72. Harney, M. B.; Pant, R. R.; Fulmer, P. A.; Wynne, J. H. Surface Self-Concentrating Amphiphilic Quaternary Ammonium Biocides as Coating Additives. *ACS Appl. Mater. Interfaces* **2009**, *1*, 39-41.
73. Pant, R. R.; Fulmer, P. A.; Harney, M. B.; Buckley, J. P.; Wynne, J. H. Synthesis and biocidal efficacy of self-spreading polydimethylsiloxane oligomers possessing oxyethylene-functionalized quaternary ammoniums. *J. Appl. Polym. Sci.* **2009**, *113*, 2397-2403.
74. Pant, R. R.; Rasley, B. T.; Buckley, J. P.; Lloyd, C. T.; Cozzens, R. F.; Santangelo, P. G.; Wynne, J. H. Synthesis, mobility study and antimicrobial evaluation of novel self-spreading ionic silicone oligomers. *J. Appl. Polym. Sci.* **2007**, *104*, 2954-2964.
75. Fulmer, P. A.; Lundin, J. G.; Wynne, J. H. Development of Antimicrobial Peptides (AMPs) for Use in Self-Decontaminating Coatings. *ACS Appl. Mater. Interfaces* **2010**, *2*, 1266-1270.
76. McCluskey, D. M.; Smith, T. N.; Madasu, P. K.; Coumbe, C. E.; Mackey, M. A.; Fulmer, P. A.; Wynne, J. H.; Stevenson, S.; Phillips, J. P. Evidence for Singlet-Oxygen Generation and Biocidal Activity in Photoresponsive Metallic Nitride Fullerene-Polymer Adhesive Films. *ACS Appl. Mater. Interfaces* **2009**, *1*, 882-887.
77. Arbogast, J. W.; Darmany, A. P.; Foote, C. S.; Diederich, F. N.; Whetten, R. L.; Rubin, Y.; Alvarez, M. M.; Anz, S. J. Photophysical properties of sixty atom carbon molecule (C₆₀). *The Journal of Physical Chemistry* **1991**, *95*, 11-12.
78. Nagano, T.; Arakane, K.; Ryu, A.; Masunaga, T.; Shinmoto, K.; Mashiko, S.; Hirobe, M. Comparison of singlet oxygen production efficiency of C₆₀ with other photosensitizers, based on 1268 nm emission. *Chem. Pharm. Bull.* **1994**, *42*, 2291-2294.
79. Pichler, K.; Graham, S.; Gelsen, O. M.; Friend, R. H.; Romanow, W. J.; McCauley Jr., J. P.; Coustel, N.; Fischer, J. E.; Smith, A. B. Photophysical properties of solid films of fullerene, C₆₀. *J. Phys.: Condens. Matter* **1991**, *3*, 9259-9270.
80. Wasielewski, M. R.; O'Neil, M. P.; Lykke, K. R.; Pellin, M. J.; Gruen, D. M. Triplet states of fullerenes C₆₀ and C₇₀. Electron paramagnetic resonance

- spectra, photophysics, and electronic structures. *J. Am. Chem. Soc.* **1991**, *113*, 2774-2776.
81. Dimitrijevic, N. M.; Kamat, P. V. Triplet excited state behavior of fullerenes: pulse radiolysis and laser flash photolysis of fullerenes (C₆₀ and C₇₀) in benzene. *The Journal of Physical Chemistry* **1992**, *96*, 4811-4814.
 82. Bagrov, I. V.; Belousova, I. M.; Danilov, O. B.; Ermakov, A. V.; Grenishin, A. S.; Kiselev, V. M.; Kislyakov, I. M.; Murav'Eva, T. D.; Sosnov, E. N.; Videnichev, D. A. Singlet oxygen generation processes in solutions of fullerenes in carbon tetrachloride. *Fullerenes Nanotubes and Carbon Nanostructures* **2008**, *16*, 675-681.
 83. Orfanopoulos, M.; Kambourakis, S. Chemical evidence of singlet oxygen production from C₆₀ and C₇₀ in aqueous and other polar media. *Tetrahedron Lett.* **1995**, *36*, 435-438.
 84. Yamakoshi, Y.; Umezawa, N.; Ryu, A.; Arakane, K.; Miyata, N.; Goda, Y.; Masumizu, T.; Nagano, T. Active Oxygen Species Generated from Photoexcited Fullerene (C₆₀) as Potential Medicines: O₂ - . versus ¹O₂. *J. Am. Chem. Soc.* **2003**, *125*, 12803-12809.
 85. Hotze, E. M.; Labille, J.; Alvarez, P.; Wiesner, M. R. Mechanisms of Photochemistry and Reactive Oxygen Production by Fullerene Suspensions in Water. *Environ. Sci. Technol.* **2008**, *42*, 4175-4180.
 86. Haufler, R. E.; Wang, L.-S.; Chibante, L. P. F.; Jin, C.; Conceicao, J.; Chai, Y.; Smalley, R. E. Fullerene triplet state production and decay: R2PI probes of C₆₀ and C₇₀ in a supersonic beam. *Chem. Phys. Lett.* **1991**, *179*, 449-454.
 87. Fraelich, M. R.; Weisman, R. B. Triplet states of fullerene C₆₀ and C₇₀ in solution: long intrinsic lifetimes and energy pooling. *The Journal of Physical Chemistry* **1993**, *97*, 11145-11147.
 88. Lee, J.; Fortner, J. D.; Hughes, J. B.; Kim, J.-H. Photochemical Production of Reactive Oxygen Species by C₆₀ in the Aqueous Phase During UV Irradiation. *Environ. Sci. Technol.* **2007**, *41*, 2529-2535.
 89. Lee, J.; Mackeyev, Y.; Cho, M.; Li, D.; Kim, J.-H.; Wilson, L. J.; Alvarez, P. J. J. Photochemical and Antimicrobial Properties of Novel C₆₀ Derivatives in Aqueous Systems. *Environ. Sci. Technol.* **2009**, *43*, 6604-6610.
 90. Lee, J.; Yamakoshi, Y.; Hughes, J. B.; Kim, J.-H. Mechanism of C₆₀ Photoreactivity in Water: Fate of Triplet State and Radical Anion and Production of Reactive Oxygen Species. *Environ. Sci. Technol.* **2008**, *42*, 3459-3464.

91. Deguchi, S.; Alargova, R. G.; Tsujii, K. Stable Dispersions of Fullerenes, C₆₀ and C₇₀, in Water. Preparation and Characterization. *Langmuir* **2001**, *17*, 6013-6017.
92. Lyon, D. Y.; Adams, L. K.; Falkner, J. C.; Alvarez, P. J. J. Antibacterial Activity of Fullerene Water Suspensions: Effects of Preparation Method and Particle Size *Environ. Sci. Technol.* **2006**, *40*, 4360-4366.
93. Belousova, I. M.; Danilov, O. B.; Muraveva, T. D.; Kiselyakov, I. M.; Rylkov, V. V.; Krisko, T. K.; Kiselev, O. I.; Zarubaev, V. V.; Sirotkin, A. K.; Piotrovskii, L. B. Solid-phase photosensitizers based on fullerene C₆₀ for photodynamic inactivation of viruses in biological liquids. *Journal of Optical Technology (A Translation of Opticheskii Zhurnal)* **2009**, *76*, 243-250.
94. Wilson, M. Light-Activated Antimicrobial Coating for the Continuous Disinfection of Surfaces. *Infection Control and Hospital Epidemiology* **2003**, *24*, 782-784.
95. Page, K.; Wilson, M.; Parkin, I. P. Antimicrobial surfaces and their potential in reducing the role of the inanimate environment in the incidence of hospital-acquired infections. *J. Mater. Chem.* **2009**, *19*, 3818-3831.
96. Perni, S.; Piccirillo, C.; Pratten, J.; Prokopovich, P.; Chrzanowski, W.; Parkin, I. P.; Wilson, M. The antimicrobial properties of light-activated polymers containing methylene blue and gold nanoparticles. *Biomaterials* **2009**, *30*, 89-93.
97. Jensen, A. W.; Daniels, C. Fullerene-Coated Beads as Reusable Catalysts. *J. Org. Chem.* **2002**, *68*, 207-210.
98. Lee, J.; Mackeyev, Y.; Cho, M.; Wilson, L. J.; Kim, J.-H.; Alvarez, P. J. J. C₆₀ Aminofullerene Immobilized on Silica as a Visible-Light-Activated Photocatalyst. *Environ. Sci. Technol.* **2010**, *44*, 9488-9495.
99. Rekharsky, M. V.; Inoue, Y. Complexation thermodynamics of cyclodextrins. *Chem. Rev. (Washington, DC, U. S.)* **1998**, *98*, 1875-1917.
100. Pavlov, G. M.; Korneeva, E. V.; Smolina, N. A. Molecular characteristics of cyclodextrins as revealed by studies of their solutions. *Biophysics* **2009**, *54*, 450-454.
101. Li, S.; Purdy, W. C. Cyclodextrins and their applications in analytical chemistry. *Chem. Rev. (Washington, DC, U. S.)* **1992**, *92*, 1457-1470.
102. Szejtli, J. Introduction and general overview of cyclodextrin chemistry. *Chem. Rev. (Washington, DC, U. S.)* **1998**, *98*, 1743-1753.

103. Dawson, B. The structure of the 9(18)-heteropoly anion in potassium 9(18)-tungstophosphate, $K_6(P_2W_{18}O_{62}) \cdot 14H_2O$. *Acta Crystallographica* **1953**, *6*, 113-126.
104. Hill, C. L.; Prosser-McCartha, C. M. Homogeneous catalysis by transition metal oxygen anion clusters. *Coord. Chem. Rev.* **1995**, *143*, 407-455.
105. Long, D. L.; Burkholder, E.; Cronin, L. Polyoxometalate clusters, nanostructures and materials: From self assembly to designer materials and devices. *Chem. Soc. Rev.* **2007**, *36*, 105-121.
106. Keggin, J. F. Structure of the crystals of 12-phosphotungstic acid. *Nature* **1933**, *132*, 351-351.
107. Fox, M. A.; Cardona, R.; Gaillard, E. Photoactivation of metal oxide surfaces: photocatalyzed oxidation of alcohols by heteropolytungstates. *J. Am. Chem. Soc.* **1987**, *109*, 6347-6354.
108. Takashima, T.; Nakamura, R.; Hashimoto, K. Visible Light Sensitive Metal Oxide Nanocluster Photocatalysts: Photo-Induced Charge Transfer from Ce(III) to Keggin-Type Polyoxotungstates. *J. Phys. Chem. C* **2009**, *113*, 17247-17253.
109. Bandwar, R. P.; Rao, C. P. Transition-metal saccharide chemistry: Synthesis and characterization of D-glucose, D-fructose, D-galactose, D-xylose, D-ribose, and maltose complexes of Ni(II). *Carbohydr. Res.* **1997**, *297*, 341-346.
110. Fugedi, P. Synthesis of heptakis(6-O-tert-butyltrimethylsilyl)cyclomaltoheptaose and octakis(6-O-tert-butyltrimethylsilyl)cyclomalto-octaose. *Carbohydr. Res.* **1989**, *192*, 366-369.
111. Takeo, K.; Uemura, K.; Mitoh, H. Derivatives of alpha-cyclodextrin and the synthesis of 6-O-alpha-D-glucopyranosyl-alpha-cyclodextrin. *J. Carbohydr. Chem.* **1988**, *7*, 293-308.
112. Tavana, H.; Neumann, A. W. Recent progress in the determination of solid surface tensions from contact angles. *Adv. Colloid Interface Sci.* **2007**, *132*, 1-32.
113. Zisman W, A., Relation of the Equilibrium Contact Angle to Liquid and Solid Constitution. In *Contact Angle, Wettability, and Adhesion*, American Chemical Society: 1964; Vol. 43, pp 1-51.
114. Owens, D. K.; Wendt, R. C. Estimation of the surface free energy of polymers. *J. Appl. Polym. Sci.* **1969**, *13*, 1741-1747.

115. Young, T. An Essay on the Cohesion of Fluids. *Philos. Trans. R. Soc. London* **1805**, *95*, 65-87.
116. Crankovic, G. M. *ASM Handbook, Volume 10 - Materials Characterization*. ASM International: 1986.
117. Lyon, D. K.; Miller, W. K.; Novet, T.; Domaille, P. J.; Evitt, E.; Johnson, D. C.; Finke, R. G. Highly oxidation resistant inorganic-porphyrin analog polyoxometalate oxidation catalysts. 1. The synthesis and characterization of aqueous-soluble potassium salts of $a_2-P_2W_{17}O_{61}(M^{n+} OH_2)^{(n-10)}$ and organic solvent soluble tetra-n-butylammonium salts of $a_2-P_2W_{17}O_{61}(M^{n+} Br)^{(n-11)}$ ($M = Mn^{3+}, Fe^{3+}, Co^{2+}, Ni^{2+}, Cu^{2+}$). *J. Am. Chem. Soc.* **1991**, *113*, 7209-7221.
118. Pichon, C.; Dolbee, A.; Mialane, P.; Marrot, J.; Rivire, E.; Goral, M.; Zynek, M.; McCormac, T.; Borshch, S. A.; Zueva, E.; Sacheresse, F. Fe₂ and Fe₄ clusters encapsulated in vacant polyoxotungstates: Hydrothermal synthesis, magnetic and electrochemical properties, and DFT calculations. *Chem.-Eur. J.* **2008**, *14*, 3189-3199.
119. Steunou, N.; Ribot, F.; Boubekeur, K.; Maquet, J.; Sanchez, C. Ketones as an oxidation source for the synthesis of titanium-oxo-organ clusters. *New J. Chem.* **1999**, *23*, 1079-1086.

Curriculum Vitae

Jeffrey Lundin is a burgeoning research chemist with experience in both high output corporate diagnostic testing and world-class scientific research.

Professional Interests: Coatings, functionalized coatings, coating application, chemical warfare agents, chemical decontamination, self-decontaminating coatings, chemical simulants, pesticides, surface chemistry, surface energy, surface analysis, C₆₀ fullerenes, photocatalysis.

Education:

George Mason University, May 2011 M.S. Chemistry

University at Albany, State University of New York, May 2007 B.S. Biochemistry and Molecular Biology

University at Albany, State University of New York, May 2007 B.A. European History

Work Experience:

2009–present; U.S. Naval Research Laboratory; Research Chemist

- Formulated a series of self-decontaminating coatings
- Characterized coatings by contact angle analysis, DSC, SEM, and FTIR-ATR
- Developed novel isothermal chamber and investigated photocatalytic activity

2008–2009; Quest Diagnostics Nichols Institute; Medical Technologist II

- Kidney stone analysis utilizing infrared spectroscopy and microscopy
- Serum immunoglobulin testing on Behring nephelometer
- Measured red blood cell fragility using UV-visible spectrometry

2007; University at Albany, Chemistry Dept.; Chemistry Study Group Instructor

- Organized the general chemistry review course
- Provided individual tutoring to students
- Taught large group review sessions

Publications and Presentations:

- 1 Refereed publication
- 1 Oral presentation
- 3 Non-refereed publications
- 1 International presentation
- 11 Conference presentations